



The author(s) shown below used Federal funding provided by the U.S. Department of Justice to prepare the following resource:

Document Title: The Development of An Objective Approach to the Characterization and Interpretation of Paint Evidence by SEM/EDS

Author(s): Christopher S. Palenik, Ph.D.

Document Number: 304615

Date Received: April 2022

Award Number: 2017-IJ-CX-0027

This resource has not been published by the U.S. Department of Justice. This resource is being made publicly available through the Office of Justice Programs' National Criminal Justice Reference Service.

Opinions or points of view expressed are those of the author(s) and do not necessarily reflect the official position or policies of the U.S. Department of Justice.

Final Report

The development of an objective approach to the characterization and interpretation of paint evidence by SEM/EDS

Prepared for:

National Institute of Justice

Grant Number: NIJ 2017-IJ-CX-0027
Recipient Organization: Microtrace LLC
Microtrace Project Number: MT18-0001
PI: Christopher S. Palenik, Ph.D.
Grant Period: 01/01/2018 to 06/30/2021
Final Report: Yes

Christopher S. Palenik, Ph.D.
Research Microscopist
cpalenik@microtrace.com

Microtrace—
790 Fletcher Drive
Elgin, IL 60123-4755

847.742.9909 (p)
847.742.2160 (f)
www.microtrace.com

DUNS: / EIN:

TABLE OF CONTENTS

Introduction.....	3
Major Research Objectives.....	4
Objective 1. Evaluation of Analytical Variables.....	5
Objective 1a. Reproducibility of EDS spectra (Counts).....	5
Results and Conclusions.....	7
Objective 1b: Reproducibility of EDS spectra (layer heterogeneity and analytical area).....	9
Results and Discussion.....	10
Examining the data in spectral space.....	12
Combining multiple spectra to achieve more representative spectra.....	13
Conclusions.....	14
Objective 1c: Paint layer edge effects on EDS spectra.....	15
Results and Discussion.....	16
Empirical data.....	16
Monte Carlo simulations.....	17
Conclusion.....	18
Objective 3: The significance and variability of elemental profiles automotive paints.....	19
Method.....	20
Results.....	21
Clearcoats.....	22
Basecoats and Tinted Clearcoats.....	23
Primers.....	24
Discussion.....	25
Association between color and elemental composition.....	27
Basecoats and tinted clear coats.....	27
Primers and Coordinated Primers.....	27
Conclusions.....	28
Impact.....	29
Impact on the Criminal Justice System.....	29
Contributions to Crime Laboratories.....	29
Impact on Technology Transfer.....	29
References.....	30
Data sets generated.....	31
Participants and Other Collaborating Organizations.....	33
Individuals Who Have Worked on This Project.....	33
Artifacts.....	33
Publications/ Presentations.....	33
Dissemination.....	35
Figures.....	36

INTRODUCTION

Paint is a common form of trace evidence because it can easily be transferred during the forcible contact between objects and people. The analysis of paint has reached routine status in most state, local, and federal crime laboratories. There are many instrumental methods utilized for the forensic comparison of questioned and known paint samples. Scanning electron microscopy coupled with energy dispersive x-ray spectrometry (SEM-EDS) is a well-established technique for the microscopical and elemental analysis of macro- and microscopic materials. The elemental analysis of vehicle paints is commonly performed by rastering or overscanning the electron beam over selected regions of both questioned and known paint samples. The comparison is then assessed based on element presence/absence and relative abundance criteria.

The assessment of this elemental comparison is challenging for various reasons. The paints and coatings used in the automotive industry are inherently complex mixtures of various organic and inorganic components. The matrix of a paint can be composed of particles that span a range of sizes. Such differences raise various analytical and interpretive challenges. A review of the published scientific research and standardized methods (e.g., ASTM paint-related methods) shows that many of these topics are unexplored. For example, studies that address sample preparation, instrumental data collection conditions, and interpretation of EDS data in the context of automotive paint comparisons are extremely limited. Yet advances in SEM/EDS instrumentation, data collection, and data processing have advanced dramatically in the past two decades. This research focuses on exploring these topics in a systematic manner.

This report is designed to give an overview of findings; however, the full extent of these findings and their interpretation in the context of forensic analysis will be published in a series of articles that are in preparation.

MAJOR RESEARCH OBJECTIVES

The overall goal of this research was to improve the fundamental basis underlying the elemental analysis and comparison of paint by SEM/EDS. The research was divided into the following sub-projects:

1. Analytical variables. The current ASTM guide (1) notes certain variables that impact the elemental analysis of paint samples by SEM/EDS. This list is limited and those variables which are addressed are not particularly well constrained. This research has evaluated the practical impact of sample preparation and instrument variables on the obtained analytical results.
2. Elementals detected. In this research, 300 automotive paint samples consisting of ~1300 layers passenger vehicles were analyzed using SEM-EDS. One method of data evaluation was to develop an understanding of the elements that were detected in these paints as a function of the layer in which they were detected. A survey of this type did not previously exist.
3. Data interpretation. The current method of comparing EDS data collected from forensic paint samples clearly works, as it has been utilized in numerous peer reviewed research studies. This research has explores several methods of interpretation and has compare them to each other to evaluate the pros and cons of

each method. The issue of data interpretation will be discussed throughout the summaries of the previous research goals.

OBJECTIVE 1. EVALUATION OF ANALYTICAL VARIABLES

There is no doubt that the forensic comparison of paint based upon elemental analysis is probative. While both the theoretical underpinnings for the elemental analysis of materials by SEM/EDS and the practical method for the comparison of forensic paint samples have been well studied, the theoretical and practical approaches have never been married. This is manifest in the present ASTM guide for the forensic comparison of paint by SEM/EDS, which offers little guidance regarding the selection of analytical variables (1). Here we have investigated parameters that impact the reproducibility of EDS spectra that are collected:

- The impact that the total number of counts in a spectrum has on the reproducibility of the spectrum for a given type of paint layer.
- The relationship between the size of the analytical area relative to the bulk composition of a given layer.
- The impact that compositionally distinct adjacent paint layers can have the EDS spectra for each layer.
- The impact of sample preparation methods.

OBJECTIVE 1A. REPRODUCIBILITY OF EDS SPECTRA (COUNTS)

Automotive paint layers are inherently complex mixtures of components that all contribute to the overall elemental profile determined by SEM/EDS. An important step in the analysis and comparison of questioned and known paint sources is to acquire reproducible EDS spectra

Microtrace —

from each layer of each sample (Figure 1). To explore this topic, thirteen paint layers spanning a range of textures and compositions were analyzed with a fixed area and different collection times to target a range of total spectrum counts.

Small portions ($\sim 3 \times 6 \text{ mm}^2$) of each paint sample were excised from their substrate (metal or polymer backing) using clean forceps and razor blades. The paint chips were mounted in a blue-light curing acrylic block and cross-sectioned using a Leica UCT Ultracut ultramicrotome with a diamond knife. This decision was made after evaluating the surface of various preparation methods including the often used “stair step” method (Figures 2 and 3) and other methods such as ultramicrotomy. Evaluation of these methods by a combination of surface roughness measurements and the resulting EDS spectra suggested that solid blocks faced by ultramicrotomy offered advantages over the traditional stair-step method used in many forensic laboratories. Preparation by microtomy produces samples that are flat and largely free of surface topography. These characteristics are highly desirable for accurate and reproducible elemental analysis by microbeam techniques. In addition to the quality of EDS data, the sectioned surface allows for detailed assessment of layer structure and filler particle morphology and distribution.

A thin ($\sim 8\text{-}10 \text{ nm}$) layer of carbon was evaporated onto the samples to reduce charging by the electron beam. A JEOL JSM-7100F field-emission scanning electron microscope with an Oxford X-Max 50 mm^2 SDD energy dispersive x-ray spectrometer was used to analyze the paint samples. The normalized elemental wt. % values for each spectrum were calculated using Oxford Aztec standardless quantitation algorithms. The data was filtered and evaluated using a combination of R (3,4) and Microsoft Excel.

The goal of this aspect of the research was to develop a basic understanding of the number x-ray counts in a single spectrum needed to achieve precise element wt. % calculations for an individual spectrum. The total counts in a given spectrum was chosen as a method of assessing the quality and stability of individual spectra because it is less dependent on instrument and analytical conditions than spectra collected on the basis of other termination criteria such as live time thresholds. Here we collected three replicate EDS spectra for eight conditions that differed in the total counts per spectrum. We analyzed 13 different paint layers for this study. The selected spectrum count conditions were: 50K, 100K, 250K, 500K, 750K, 1M, 1.5M, and 3M total counts. The spectra for each of the analyses were collected at 20 KV with a dead-time values that ranged from 5-15% (5). The electron beam was rastered over the same area (approximately 532 μm^2) for a given layer for each of the eight total spectrum count conditions.

RESULTS AND CONCLUSIONS

A summary of the results for the total spectrum counts study are shown graphically in Figure 4. The measurement percent relative standard deviation (% RSD) is plotted against the measured element wt. % values for all 13 layers analyzed. The elements that are typically of interest in forensic paint comparisons (those derived primarily from pigments and fillers) range from ~0.1-35 wt. %. The analyses at wt. % values greater than ~50% are carbon and oxygen. These elements had the lowest % RSD values since they are derived primarily from the organic binders and thus present at high wt. % levels. In addition, the carbon wt. % values are also influenced by the thin layer of conductive carbon that was applied to all samples. As expected, the % RSD is inversely proportional to the measured element wt. %. In addition, the

data demonstrate lower element % RSD values are achieved in spectra that contain more total counts.

To compare the measurement performance for the spectra, which were collected at different total counts, the element wt. % that was required to achieve RSD values below 5% was assessed (Table 1). Note the dramatic improvement in measurement precision when the spectrum contains $\geq 250\text{K}$ counts as opposed to $\leq 100\text{K}$ counts. This significant improvement in measurement precision is largely due to acquiring sufficient x-ray counts to achieve stable spectra for calculating element peak-to-background ratios. For spectra that contain $\geq 250\text{K}$ total counts, detected elements must be present at levels above ~ 4 wt. % for the measurement %RSD to drop below 5%. These empirical data may inform case-workers of the expected measurement uncertainty for differing paint composition (element wt. % values) and EDS collection parameter combinations.

Table 1. Approximate element wt. % to achieve measurement %RSD values below 5%.

Total Spectrum Counts	Approximate element wt. % value at which measurement RSD primarily remained below 5%
50K	33%
100K	21%
250K	4.3%
500K	3.5%
750K	1.3%
1M	0.7%
3M	0.5%

OBJECTIVE 1B: REPRODUCIBILITY OF EDS SPECTRA (LAYER HETEROGENEITY AND ANALYTICAL AREA)

The goal of this aspect of the research was to better understand the impact of the size of the region selected for analysis by EDS to sufficiently represent the composition of the paint layer as a whole. To address this question, nine layers (Figures 5 and 6) were selected based on their significant differences in elemental compositions (presence/ absence and abundance criteria) and the particle size distribution of the pigments/ fillers. This variability is beneficial as these samples serve as a robust test set to assess the elemental heterogeneity and thus provide reliable guidance for the analytical parameters required to collect reproducible EDS data.

A defined region measuring $9,600 \mu\text{m}^2$ was measured for each of the nine layers. The elemental composition of this large region (which is assumed to be much larger than is typically analyzed in most case-work samples) will be treated as the parent/bulk elemental composition of the paint layer and serve as “ground truth” for the set of experiments. These regions were subsequently divided (by a factor of 2 per subset) into progressively smaller regions (Figure 7). This resulted in 5 subsets each capturing an area of: $4,800 \mu\text{m}^2$ (n=2), $2,400 \mu\text{m}^2$ (n=4), $1,200 \mu\text{m}^2$ (n=8), $600 \mu\text{m}^2$ (n=16), or $300 \mu\text{m}^2$ (n=32). The locations of the smaller regions were drawn within the parent spectrum area; thus, the individual replicate regions sum to the parent spectrum area. The instrument conditions for the analyses were held constant: 20 kV accelerating voltage, 500,000 counts/ spectrum (see results from Objective 2a. Assessing the reproducibility of EDS spectra as a function of number of counts in acquired EDS spectra.) and spot size/ current value of 10 which yielded a dead-time of 5-15%.

RESULTS AND DISCUSSION

To aid in data integration and interpretation, the nine layers will be discussed in reference to their apparent heterogeneity which was assessed by visual examination of back-scatter electron images of the individual layers (Figures 5 and 6). The three categories are termed “low-”, “medium-”, and “high-grade”. Layers 80333 OU2, 80375 OT1, 80406 OT3, and 80390 OU2 are classified as low-grade, layers 80406 OT1, 80390 OU1, 80333 OU1, and 80333 OT1 are medium-grade, and layer 80375 OT2 is considered high-grade (Figure 5). Note the “low-grade” category is still significantly more visually heterogeneous than is observed in clear coat layer (those that do not contain effect pigments), which are not part of this study.

The differences between the calculated element wt. % values for each replicate spectrum relative to its parent composition for four analytical areas (2400, 1200, 600, and 300 μm^2) for representative paint layers are shown in Figures 8 - 12. In general, the absolute differences between the calculated wt. % values for the individual spectra relative to the parent spectra increase with decreasing analytical area and decreasing element wt. %. However, as can be seen for spectra for the low heterogeneity group (Figure 8 and 9), the absolute difference between any one spectrum (regardless of its size) and the parent is generally on the order of a few wt. % (typically 1-3%). The largest differences are most commonly observed for the carbon and oxygen (recall that the samples are also carbon coated). This is expected as these are the most abundant, as such the measurement error for these elements has a greater impact on absolute changes in the calculated wt. % than on lower abundance elements. These lighter elements are also the most prone to beam damage, which could result in changes in these

elements within the analytical area. Rastering the electron beam over large areas, as was done in this study, should help to minimize this effect.

Examination of the element wt. % values from the medium grade group shows more variability and increased range in differences from their parent spectra than was observed the low-grade group. However, for any single spectrum the element wt. % difference between it and the parent is on the order of only 2-4 wt. % (Figure 9 and 10). Carbon and oxygen again show the largest difference relative to the parent spectra. However, while the examination of the element wt. % values for 80406 OT1 can show more variability in the measured concentrations of aluminum (Figure 10) a) this difference is still less than ~8 wt. % for aluminum when using the smallest rastered area ($300 \mu\text{m}^2$) under ~2 wt. % when using a larger rastered area ($2400 \mu\text{m}^2$). This observation is expected as there are large (~20 μm long) Al flakes dispersed throughout the finer matrix of the layer (Figure 6). Thus, depending on the presence/ proportion of these Al flakes in the analytical area, wt. % values can fluctuate; however, this textural distinction may also serve as a useful point of comparison.

Layer 80375 OT2 which represents the highest degree of heterogeneity is shown in Figure 5. As expected, this layer shows the most variability for the individual spectra in the data set. However, the difference between the wt. % values for most elements in any individual spectrum are generally 2-5 wt. % (Figure 11). However, both calcium and barium, can vary by larger amounts. The source of this variation is due to the higher concentration of this component and the larger particles (~20 μm) of calcium carbonate (CaCO_3) and barite (BaSO_4) present in the layer. However, as the analytical area increases, this variation in wt. %

decreases, and at analytical areas of 1200 and 2400 μm^2 , the variation in these elements, which are present as larger inclusions is on the order of ~ 2 wt. % or less.

Examining the data in spectral space

The data in this sub-study have been presented by transforming the EDS spectra into compositional data (wt. percentages). This was performed to aid in the presentation and analysis of readily relatable and quantifiable metrics. In forensic science, it is common practice for case-workers to visually examine and overlay individual spectra as part of their K-Q comparisons (1,6). To link both of these data spaces, we calculated the 95% data intervals for the replicate EDS spectra from representative paint layers from each of the three heterogeneity groups at three different analytical area window sizes (1200, 600, and 300 μm^2). The results from these analyses are shown in Figures 13-21.

Examination of the data provides a framework to understand the potential variability in a single EDS spectrum for a given paint layer. For low heterogeneity layers (Figures 13 -15), the EDS spectra and their associated wt. % values show little variation. For paint layers that show low-grade heterogeneity, the analytical area needed to capture a representative EDS spectrum is small. The EDS spectra collected from 300 -1200 μm^2 areas are indistinguishable from their parent spectrum (Figure 13 - 15).

For paint layers that are considered to have medium-grade heterogeneity, they result in broader 95% data windows (Figure 16 -18). However, the spectra that were collected from 1200 μm^2 areas are indistinguishable from their parent spectrum (Figure 16). The spectra from the 600 μm^2 areas show some variation, but do not display substantial differences (Figure 17). The spectra collected from 300 μm^2 areas show broader 95% data ranges (Figure 18) than was

Microtrace —

observed for the two larger area spectra. This observation suggests that a single spectrum collected from a 300 μm^2 area may not be an adequate representation of the elemental composition range of the paint layer under investigation.

Layer 80375 OT2, which shows a high level of heterogeneity, the windows that contain 95% of the data are more broad (greater difference between the 2.5 and 97.5 percentiles) for all three analysis areas (Figures 19 -21). The spectra that were collected from 1200 μm^2 areas show some differences to their parent spectrum (Figure 20); however, these differences are not necessarily significant (since significance will depend upon criteria of comparison). As smaller areas are used, the variation becomes larger. The spectra from the 600 μm^2 and 300 μm^2 areas show increasingly broad 95% data ranges (Figure 21). This observation suggests that a single spectrum collected from either a 600 or 300 μm^2 area may not be an adequate representation of the paint layer under investigation. Note; however, that a 600 square micrometer area equates to a roughly 25 μm square analytical box, while that of a 300 square micrometer area equates to a roughly 17 μm square analytical area, which are typically small compared to the analytical area available for many forensic paint comparisons.

Combining multiple spectra to achieve more representative spectra

The ASTM E2809-13 (1) guideline for forensic paint analysis discusses the collection of multiple spectra for a given layer to obtain more representative analyses of paint layers under investigation. This statement is provided but it is not supported by any published scientific studies to demonstrate its validity. The goal of this aspect of the research was to test the utility of combining multiple spectra from a single layer to achieve a more accurate representation of the parent paint composition. On the basis of the previously discussed experiments, we made

combinations of the 600 and 300 μm^2 spectra to achieve 1200 μm^2 of analyzed area. For each of the nine layers analyzed, we averaged all possible combinations of two 600 μm^2 spectra or four 300 μm^2 sized spectra. This resulted in 120 combinations for the 600 μm^2 spectra and 35690 combinations for the 300 μm^2 spectra. The 2.5 and 97.5 percentile ranges were calculated for each element. The results from these combinations for three layers (one representing each of the three heterogeneity grades) are shown in Figure 22-27. The area between the two curves contains 95% of the data. As can be seen, combining multiple spectra does result in data that are closer to the parent composition. However, averaging multiple spectra to achieve the goal of 1200 μm^2 of analyzed area does not achieve the closeness to the bulk composition as is observed in a single spectrum of the same area. Thus, acquiring a spectrum from the largest achievable area (as a single spectrum) is recommended versus averaging multiple smaller area spectra together. However, elements present at trace levels may be missed. Thus, a combination large area with targeted analyses of several smaller areas may provide complementary information to aide in paint layer characterization and forensic comparison.

CONCLUSIONS

The layers selected and analyzed in this study were chosen to serve as analogs for common vehicle paints that may be seen in casework. Thus, the data presented may provide a framework in which to understand the potential intra-sample variability in the spectra acquired for the paint layers in forensic investigations. Here we show the intra-sample variability in the EDS spectra and associated element wt. % values are impacted by the size of the analysis area and the heterogeneity of the paint layer. The data for all layers analyzed show a clear inverse

trend relating the size of the analysis area for an EDS spectrum and its ability to capture the bulk composition of the paint layer. On the basis of this study, we *recommend* for paint layers that display medium- to high-grade heterogeneity (as assessed by examination of BSE images) that at least 1,200 μm^2 areas are analyzed and the spectra contain a minimum of 500K total counts. If this area is not available to be analyzed in a single spectrum, the averaging of multiple spectra to achieve the 1200 μm^2 area criteria is recommended. For paint layers that display low degrees of heterogeneity, analysis areas of 300-600 μm^2 may be sufficient. In case-work it is recommended to analyze the known sample in detail to understand the potential intra-sample variability that may be present. *It is important to note that each paint case is unique and the recommended analysis conditions may be adjusted according to the nature of the samples, the analyst's discretion, and the parameters of comparison that are selected.*

OBJECTIVE 1C: PAINT LAYER EDGE EFFECTS ON EDS SPECTRA

The ability to separate and consequently avoid signal (x-ray) contributions from adjacent layers to the signal of a targeted layer of the analysis is an important consideration for paint layer characterization. A major element from an adjacent layer can potentially occur as a minor or trace element in the EDS spectrum for the targeted layer, which will consequently lead to increased uncertainty in the measured compositional profile. Systematic analytical experiments have been carried out to investigate the occurrence and potential impact that mixed layer signals can have in automotive paint samples. The aim of this research was to determine the distance to an adjacent layer that must be kept in order to avoid mixed signals and, if it is possible, constrain a “universal” guide line to prevent adjacent layer contamination when analyzing layered paint samples.

Empirical analyses were performed using a JEOL JSM-649OLV scanning electron microscope coupled to a Thermo Scientific NORAN System for x-ray microanalysis (SEM-EDS).

Selected sample areas were mapped at an accelerating voltage of 20 kV with a spot size of 65 and a fixed EDS time constant of 3 (equal to ~12000 cps throughput). Elemental maps were acquired with a resolution of 512*384 pixels.

To further support experimental results, *in silico* Monte Carlo simulations have been performed in order to statistically investigate distance to an adjacent layer where mixed signals occur. In order to perform these simulations, the open-source program NIST DTSA-II (Version: Jupiter 2017-11-06) was used. General chemical compositions for clear coats and color coats were derived from published formulations (2). These synthetic layers (i.e., Clear Coat and Color Coat) were chosen for Monte Carlo simulations.

RESULTS AND DISCUSSION

Empirical data

Results show that in almost every sample, independent of the layer interface or the element the first indication of signal contribution from an adjacent layer can be detected at a 5 to 3 μm to the adjacent layer (Figure 28). It was noted that variable distances were calculated for the same element at different interfaces or paint layers, as well as for different elements at the same interface. It is also important to note that the size and shape of analytical interaction volume with the sample is dependent on the element of interest, as well as the matrices of the layers forming the interface. For example, high-atomic-number targets will have a reduced x-ray penetration when compared to lower-atomic-number targets. In the same matrix, an element with a high-atomic-number will have a noticeable smaller interaction volume compared to a

low-atomic-number element. However, no systematic variations were found between the calculated, necessary distances to prevent adjacent layer contamination and for example the atomic number of the investigated elements. This is most likely because the experiments were performed on actual paint layer samples and not on idealized samples, providing two homogeneous layers with a perfectly straight interface, but rather heterogeneous samples with irregular pigment distribution (size, shape, and composition) and an imperfect interface. Furthermore, no information exists on how the layer interfaces are orientated and for example pigments are distributed within depth of actual samples. Considering the various sources of uncertainty, results for the distances that must be kept to minimize a signal contribution from an adjacent paint layer sample, suggest that 3-5 μm is a reasonable rule of thumb; however, at even smaller margins, the contributions from adjacent layers may not appreciably affect analytical results.

Monte Carlo simulations

To further test the results of the empirical study, Monte Carlo simulations were performed. The focus of this aspect of the research was not to precisely simulate the measurements of the automotive paint samples (i.e., compositionally wise and texturally wise); but rather to determine a generalized estimate for the distance at which signal from adjacent layers could be detected based on average compositional estimates of different layer types. Results from Monte Carlo simulations targeting the detection of Al in the clear coat at variable distances to the Al-metal interface, as well as a homogeneous Al-bearing color coat are displayed in Figure 29. In both cases (i.e., clear coat – metal and clear coat - color coat interface) the first detection of Al X-rays occurs at 5 μm distance to the interface; however, at this point the contribution is

generally well under 1 %. However, the Al signal contributions from the adjacent layers to measurements targeting the clear coat are only detected at a distance of $\sim 3 \mu\text{m}$ to the interface (detection $> 1 \%$). These results are in good agreement with our empirical analytical study of automotive paint layer samples (Figure 28). Besides this finding a second important observation can be made in the results of the performed Monte Carlo Simulations. In the Clear Coat at a distance of $\sim 8 \mu\text{m}$ to the interface C, N, O and Si are at a detection of 100%, reflecting a certain homogeneous concentration of these elements in that layer. However, closer to the interface ($\sim 6 \mu\text{m}$) C, N, O and Si show a decrease in the emitted X-ray signal. The consequence of this disproportional signal decrease is an actual change in the counts resulting in different calculated concentration for these elements in the exact same material close to an interface when compared to measurement taken in an area with no contribution (e.g., at 7-8 μm away) from an interface.

CONCLUSION

In this study we performed SEM-EDS analysis for layered automotive paint samples, as well as Monte Carlo simulations to investigate the distance that must be kept to adjacent layers when selecting the area for analysis to avoid a mixed EDS signal. This issue arises from the well-known divergence between the targeted area for analysis and the resulting excited sample volume that will produce X-rays. The combined results of the analytical investigation of the automotive paint samples and the Monte Carlo simulations are very consistent in that they show that a conservative estimate of 5 μm margin to an interface avoids any significant signal contributions from the adjacent layer. The consistency of the results is highly encouraging in that it shows that it is possible to confidently separate or exclude a signal from an adjacent

layer to the analysis. With this said, a 5 μm distance to an adjacent layer may prevent challenges when working with thin automotive paint layers.

OBJECTIVE 3: THE SIGNIFICANCE AND VARIABILITY OF ELEMENTAL PROFILES AUTOMOTIVE PAINTS

Scanning electron microscopy coupled with energy dispersive x-ray spectrometry (SEM-EDS) is a well-established technique for the microscopical and elemental analysis of macro- and microscopic materials. Forensic examinations of paint using SEM-EDS/ microprobe first began in the early 1970's (7), when the technique was first being incorporated into crime laboratories. Since this time, SEM-EDS has been routinely utilized for the examination and comparison of paint evidence. However, there are no published research studies showing the abundance and variability of the element profiles of automotive paint. In addition, the automotive paint industry is continuing to change as advances in technology are coming online. Thus, there is a need to assess the current elemental profile populations of vehicle present in the consumer market. As a result of these key observations, the goal of this research is to better understand the elemental profiles of modern vehicle paints and their potential correlation with layer-type (i.e., clearcoat, basecoat, and primer) and color.

For this research 300 automotive paint samples from passenger vehicles were collected (Figure 30). These samples were embedded, cross-sectioned with a microtome, and each of the nearly 1300 layers in the sample set was analyzed using SEM-EDS. The results of this research show that the elemental diversity increases from the outer layers (clearcoat) to inner layers (primers). The range in elemental composition for the analyzed paint layers is significant, spanning 28 different elements detected/quantified. The results show that with proper sample preparation

and analysis, elemental profiling is a valuable method for more complete sample characterization and comparison.

METHOD

Small portions (~3 x 6 mm²) of each paint sample were excised from their substrate (metal or polymer backing) using clean forceps and razor blades. The paint chips were mounted in a blue-light curing acrylic block and cross-sectioned using an American Optical 820 rotary microtome with a steel knife (8–10). Preparation by microtomy produces samples that are flat and largely free of surface topography. These characteristics are highly desirable because they are required for accurate and reproducible elemental analysis by microbeam techniques (11). Flat samples allow for reproducible electron beam-to-sample and x-ray emission-to-detector geometries. In addition, the sectioned surface allows for detailed assessment of layer structure and filler particle morphology and distribution (see Objective 2b: Assessing the reproducibility of EDS spectra as a function of layer heterogeneity and size of analytical region.).

A thin (~5-8 nm) coat of carbon was applied to the cut surfaces of the prepared paint blocks to reduce surface charging. The samples were analyzed using a JEOL JSM6490-LV scanning electron microscope coupled with a Thermo UltraDry SDD energy dispersive x-ray spectrometer. Each sample was magnified to fill the field of view so that the thickness of the paint chip spanned the height of the field, typically ~400-1000x. Backscattered electron imaging (BSE) was used to visualize the samples, and rectangular analysis areas were drawn on each layer, constraining the analytical area to the middle ~2/3 of the width of a given layer, when possible. This was done to reduce the potential for the elemental composition of the target layer to be influenced by that of the adjacent layers (see Objective 2b). All spectra were

collected at 20 keV for 200 live seconds, with a fixed aperture and process time (resulting in a detector dead time <10%). Each spectrum was processed using Thermo Pathfinder[®] (v1.2) to calculate the normalized concentrations, reported as weight percent (wt. %) along with measurement uncertainty (σ) values. The data was filtered and evaluated using a combination of R (3,4) and Microsoft Excel[®].

The spectra were processed by quantifying a fixed list of elements (n=28 elements), thus removing analyst variability, treating all spectra uniformly, and decreasing processing time. The list of quantified elements was developed by first utilizing the software-automation to “identify” the elements present in the population of spectra. Select spectra, containing at least one of the elements in the list, were then manually evaluated to confirm the validity of the assignment. As necessary, erroneous peak assignments were corrected and the list of detected elements was refined.

The spectra were then reprocessed to quantify the fixed list of 28 elements. The quantitative results in the form of element weight percentages (wt.%) were then evaluated to assess the presence of an element. This was accomplished by evaluating the analytical uncertainty of that result ($\text{wt.}\% > 3\sigma$) and setting detection cutoff thresholds (minimum wt. % of 0.1) for element identification. The absolute accuracy of standardless quantification was not the focus of this survey, but rather this method provided objective, uniform processing of a large data set.

RESULTS

The EDS data was evaluated to examine the element frequency and wt. % distribution in the different layer types. The spread in wt.% values for many of the detected elements showed a right skewed distribution, meaning for many elements it was more common to measure values

lower than the calculated mean. Therefore, the median value was found to be more representative of the typical concentration of each element, thus this value is reported in the following sections. The elemental abundances were categorized into two groups, major elements (median ≥ 1 wt.%) and minor elements ($0.1 \leq$ median < 1.0 wt.%). As a general trend, the paint layers become more elementally complex moving from the exterior (clearcoat) to the interior (primer layers).

Clearcoats

The clearcoat layers (n=364) in the dataset show a limited range in major-minor elemental composition (Figure 31). Four elements, C, O, N, and Si, were detected above the 1% threshold (Figure 31). Detecting such a small number of major elements is not surprising as clearcoats are protective layers intended to impart a “wet” or “glossy” appearance to the vehicle. As such, color and effect pigments, which scatter and absorb light, are not added to these layers. Note tinted clearcoats were included with the basecoat discussion below.

As expected, carbon and oxygen were detected as major elements in each clearcoat. Nitrogen was detected in 43% of the layers, and, when detected, was present exclusively as a major element (median – 5.2 wt.%, max 14.0 wt.%). Boxplots (Figure 32) show the major element wt.% distributions in clearcoat layers. The distribution of both C and O approximate normal distributions around their means with few outliers; however, the dispersion of N and Si are right skewed.

Additional elements were sporadically detected in the clearcoat layers; however, such occurrences were exclusively below 1 wt. %. These additional elements had median concentrations of ~ 0.2 wt.%, just slightly above the trace element cutoff threshold.

Microtrace —

Examination of select spectra from clearcoat layers containing these additional elements revealed that they often originate from thinner, 10-20 μm , repaint layers (i.e., from the middle of the chip). The adjacent layers in these instances were often found to contain these same elements at higher concentrations relative to the clearcoat. Thus, several of these additional elements, which are detected just above the trace element cutoff, are likely not present in the clearcoats but potential contributions from adjacent layers (see Objective 2c).

Basecoats and Tinted Clearcoats

Basecoats impart color to an automotive paint, and consequently they contain pigments and extenders. Tinted-clearcoats also impart a visual effect, sometimes described as “candied”, to the appearance of the vehicle. They utilize the same general binder chemistries as clearcoats but contain lesser amount of pigment (relative to a basecoat). The presence of pigments and extenders in these layers is expected to result in more elementally complex data compared to traditional clearcoats.

Figure 33 shows a histogram of the major and minor elements that were quantified in the basecoats and tinted clearcoats (n=415). A total of 25 elements were detected at major to minor concentrations in these layers. Sixteen elements were detected at major concentrations, and eight elements were detected in greater than 50% of the layers. Nitrogen was detected in 47% of the layers and, when detected, was present as a major element.

The quantitative values for the elements which were detected in >50% of the layers (Al, Si, P, S, Ti, and Fe) are depicted in histograms in Figure 34; this shows another representation of the wt.% distribution of these commonly detected elements. Aluminum concentrations range from ~0.1 to >20 wt.% with median value of 3.6 wt.% and a maximum of 36 wt.%. Si is typically

Microtrace —

present < 5 wt.% and had a median value of 1.2 wt.% and maximum of 16.5 wt.%. Phosphorus is typically present at very low concentrations, resulting a median concentration of 0.2 wt.%. Sulfur and Fe both show right skewed distributions, with median values of ~0.3 wt. % and maximum measured quantities of 7.1 and 7.9 wt. %, respectively. The measured Ti concentrations show the widest spread, and tend to appear either <5 wt. % or > 20 wt. %.

Primers

Of the three major layer types found in passenger vehicle paint, primers are the most elementally diverse (Figure 35). All twenty-eight of the surveyed elements were detected above trace levels in the primer layers (n=492), 18 of these elements were detected in major quantities in these layers. Primer layers were found to have the highest amount of extender pigments. This is based on the lowest C and O average wt. % values compared to the other two layer types. Consequently, this allows for a large amount of elemental variability (Figures 35-36). The measured wt. % values for several of the elements (O, Mg, Si, P, Cl, Zn, and Ba) approximate normal distributions around their calculated means for the dataset as a whole. The distributions for the majority of element are right skewed. However, the distributions for C and Ca are left skewed. Again, for the elements with skewed distributions, the median value is more representative of the “typical” wt. % value of that element.

Interestingly, the same eight elements that were detected in >50% of the basecoat layers were also present in >50% of the primer layers (Figure 36). Phosphorus is still present at typically low quantities with a measured median value of 0.2 wt.%, but had a higher maximum detected value of 3.2 wt.%. Iron shows a sharply right skewed distribution, with a median value of 0.2 wt.% and a measured maximum value of 16.8 wt.%. The titanium distribution is most different

Microtrace —

between basecoats and primer layers. Instead of a bimodal distribution, which was observed in basecoats, titanium was consistently detected at high concentrations. In primer layers, Ti had a measured median value of 9.3 wt.% and a maximum at 39.8 wt%.

DISCUSSION

The survey of elemental compositions within automotive paints, grouped by layer type (clearcoat, basecoat, and primer) provides a means for understanding the range of elements that an analyst may expect to encounter in forensic paint analyses. Such information provides a basic foundation to assess the commonality/rarity of a sample, and could assist in determining the significance of an evidentiary association. For example, this dataset demonstrates that it would not be uncommon for an analyst to detect high concentrations of titanium or iron in a basecoat, but it is less common to encounter major quantities (>1 wt.%) of calcium or copper in these same layer types. However, the forensic comparison of paint rarely hinges on the presence/ absence of single elements but more commonly utilizes the total element profile. To that end, the frequently detected elements (C, N, O, Al, Si, P, S, Ti, Ba, and Fe) would not provide significant sample discrimination from a presence/absence criterion. However, it is noteworthy that many of these elements were detected across multiple orders of magnitude (~0.1 to >10.0 wt. %). Therefore, when interpreting wt.% values or peak ratios, these elements may provide a significant amount of variation and thus may be useful for sample discrimination.

To fully understand the probative value of vehicle paint element profiles, it is important to examine how each element varies relative to each other. The elemental correlation is shown graphically in Figure 37 . Examination of this data shows that there are strong positive

correlations between Mg-Si, Ba-S, and Zn-P. It can be inferred that these identified element pairs are indirectly identifying talc, barite, and zinc phosphate respectively, which are common extenders in automotive coatings (12). In addition, there are several weak trends (correlation values ≥ 0.3) between other element pairs (e.g., Zn-Cl, Ca-P, Zn-Si, among others). The meaning (if any) of these correlations is not known. It is possible that they may provide insight into co-utilization of certain extenders, but the validity of this would require a significantly larger dataset to test this premise.

Aluminum is negatively correlated with most other elements, meaning the more Al, the less of other elements. Layers with the highest aluminum concentrations correspond to silver basecoats, which are simply binder with aluminum flake; thus, it follows that high Al concentrations result in lesser concentrations of the other elements.

Recognizing the degree of element correlation is important for assessing the rarity or commonality of an element profile. For example, detecting Ba in a paint sample essentially ensures that S will also be present. Thus, identifying both of these elements provides no new information, unless they are in some proportion that falls significantly out of the anticipated Ba:S ratio of ~ 4.28 for barite (BaSO_4), which we have not observed(13). A similar situation can be seen when measuring Zn, as P will very likely to also be detected because these two elements correlate strongly. However, Zn can occur as an oxide, thus negating the necessity of P to be present. In accordance, the detection of P does not predict the presence of Zn, as there are other P-containing paint additives.

ASSOCIATION BETWEEN COLOR AND ELEMENTAL COMPOSITION

The potential association between elemental composition and vehicle paint color for the basecoats (including tinted clearcoats) and primer layers is shown in Figures 38 - 39. As can be seen from inspection of these figures, there are minor trends or elemental signatures for some of the colors. There are also distinct differences with the element-color associations between the basecoat-tinted clear coats and the primers; consequently, these will be discussed separately.

Basecoats and tinted clear coats

Red, brown, and green paints have high amounts of Al (affect pigment). White colored layers have the highest median wt.% values for F, Cl, Ca, and Ti. Both white and blue paints have high levels of Ba. Silver and gray coats have the highest Fe median wt. % values. The blue and green colored paints have the highest levels of Cu. We interpret the Cu to be derived from copper phthalocyanine pigments. The black-colored layers have the highest median Zn wt. % values.

Primers and Coordinated Primers

There is little association between color and several of the low abundance elements (Mg, Al, Si, P, Sn, and Bi). Blue-colored primers have the highest median levels of S and Ca. Blues and blacks have the highest median levels of Cl, which we again interpret to result from the presence of chlorinated copper phthalocyanine green (which contains ~45% Cl). Blues and blacks also have the highest median wt. % values for Ba. Titanium is common in all nominal primer colors except blue. Red colored primers have high levels of Fe, which is interpreted to

be a result of iron oxide pigments. The median Zn wt. % is lowest in yellows and greens.

Strontium is significantly more abundant in red primers than all other colors.

CONCLUSIONS

The results from the elemental analysis of the nearly 1,300 individual layers shows significant elemental diversity among the layers. Based on the limited elemental diversity observed in clearcoats, elemental profiling of these layers has limited utility for the differentiation of sources. The elemental profiles of the basecoats were more diverse with a much higher total amount of non-binder derived elements in comparison to the clearcoats. The layers that had the most elemental abundance and diversity were the primer and coordinated-primer coats. This observation is understandable when one considers the function for these layers. Thus, the elemental profiles of basecoats and primer layers holds the greatest potential for sample discrimination.

The results of this research provide a framework in which one can interpret the commonality/rarity of detected and quantified elements in forensic casework involving paint transfer evidence. Here we show that there are distinct elemental trends based on both layer type and color. These are important concepts that should be taken into consideration when evaluating the elemental profiles of paint evidence. For example, measuring a high amount of Ti in black or white primers is quite common, but detecting/ quantifying high levels of Al in these same-colored paints would certainly be uncommon (provided the analyzed data set is representative of the current automobile paint population).

IMPACT

IMPACT ON THE CRIMINAL JUSTICE SYSTEM

While forensic research and casework have demonstrated that EDS analyses of paint are probative, there are numerous aspects of this analysis that could be better understood, improved, or standardized. Some aspects of these analyses have been criticized by academic scientists. One motivation for this research is to take the criticisms of the academic community, in light of the practical limitations associated with forensic analyses, to improve the basis upon which these analyses are conducted.

CONTRIBUTIONS TO CRIME LABORATORIES

In practical terms, it is anticipated that the results of this research will provide more specific guidance on numerous aspects of the elemental analysis of paint. It is anticipated that this research will directly benefit crime laboratories by improving a) the scientific basis for paint evidence, b) the overall significance of paint comparisons, and c) the investigative value of forensic paint samples. At the bench-level, it is anticipated that the results of this research, which are being prepared for publication in peer reviewed journal articles, will provide new and practical guidance to the analyst, which will improve the quality and significance of analytical results.

IMPACT ON TECHNOLOGY TRANSFER

This results of this research are intended to be directly applicable to laboratory personnel at the crime laboratory bench level. The goal is to improve the use of available technology (*i.e.*, current generation SEM/EDS systems), capabilities that are already widely available in crime laboratories. The publications and presentations at meetings will be the largest factors

encouraging technology transfer. Ultimately, we anticipate that the results from this research will be used to improve the quality of forensic casework at the bench-level.

REFERENCES

1. Standard Guide for Using Scanning Electron Microscopy/X-Ray Spectrometry in Forensic Paint Examinations 1. Available from: www.astm.org,
2. Poth U. Automotive Coatings Formulations-Chemistry, Physics, and Practices. Hannover, Germany: Vincentz Network; 2008. 237 p.
3. RStudio Team. RStudio I. RStudio: Integrated Development for R [Internet]. Boston, MA: RStudio, Inc.; 2020. Available from: <http://www.rstudio.com/>
4. R Core Team. R Foundation for Statistical Computing. R: A Language and Environment for Statistical Computing [Internet]. Vienna, Austria; 2020. Available from: <http://www.r-project.org/>
5. Newbury DE, Ritchie NWM. Performing elemental microanalysis with high accuracy and high precision by scanning electron microscopy/silicon drift detector energy-dispersive X-ray spectrometry (SEM/SDD-EDS). *J Mater Sci*. 2015 Jan;50(2):493–518.
6. ASTM Standard E1610-18. Standard Guide for Forensic Paint Analysis and Comparison. *Astm Int*. 2018;
7. Smale D. The examination of paint flakes, glass, and soils for forensic purposes, with special reference to electron probe microanalysis. *J Forensic Sci Soc*. 1973;13(1):5–15.
8. Laing DK. *InternationalL* 46 (1990) 37 - 39. 1990;46:37–9.

9. Allen TJ. Modifications to sample mounting procedures and microtome equipment for paint sectioning. *Forensic Sci Int* [Internet]. 1991 Dec;52(1):93–100. Available from: <https://linkinghub.elsevier.com/retrieve/pii/037907389190100W>
10. Groves E, Palenik CS. Applications of Blue Light-curing Acrylic Resin to Forensic Sample Preparation and Microtomy. *J Forensic Sci* [Internet]. 2016 Mar;61(2):489–93. Available from: <http://doi.wiley.com/10.1111/1556-4029.12993>
11. Goldstein JI, Newbury DE, Michael JR, Ritchie NWM, Scott JHJ, Joy DC. Scanning electron microscopy and x-ray microanalysis. Third. *Scanning Electron Microscopy and X-ray Microanalysis*. New York: Springer; 2003. 689 p.
12. Thornton J. Forensic Paint Examination. In: Saferstein R, editor. *Forensic Science Handbook, Volume 1*. 2nd ed. Upper Saddle River, NJ: Prentice Hall; 2002. p. 429–78.
13. Deer WA, Howie RA, Zussman J. *An introduction to the rock-forming minerals*. Second edition. An Introd to rock-forming Miner Second Ed. 1992;

DATA SETS GENERATED

A set of 300 automotive paint samples comprising ~1,300 individual layers were analyzed by SEM/EDS. In addition, publication-quality reflected light photomicrographs of each paint sample were collected. The sample set consists of passenger vehicles and trucks sourced from automotive repairs shops in suburban Chicago, IL, USA. The samples range from pre-1999 through 2012, span the most common nominal colors, and represent over 30 different vehicle brands

PARTICIPANTS AND OTHER COLLABORATING ORGANIZATIONS

INDIVIDUALS WHO HAVE WORKED ON THIS PROJECT

Name: Christopher S. Palenik, Ph.D.
Project Role: PI / Research Microscopist, Microtrace LLC
Residence: Illinois, USA
Foreign Collaboration: No

Name: Ethan Groves, M.S.
Project Role: Research Microscopist, Microtrace LLC
Residence: Illinois, USA
Foreign Collaboration: No

Name: Jack Hietpas, Ph.D.
Project Role: Research Microscopist, Microtrace LLC
Residence: Illinois, USA
Foreign Collaboration: No

Others providing support on this project from Microtrace include: Skip Palenik, Jason Beckert, Brendan Nytes, and Kelly Beckert, Katie White, and Otyllia Abraham.

ARTIFACTS

PUBLICATIONS/ PRESENTATIONS

- Groves, E., Michely, L., Lim, Y.C., Hietpas, J, and Palenik, C.S. (*in prep.*). Assessing the occurrence and variability of elemental profiles in multi-layered automotive coatings.
- Hietpas, J., Groves, E. and Palenik, C.S. (*in prep.*). Steps to achieve representative and reproducible SEM-EDS spectra for vehicle paints and coatings.

- Michely, L., Groves, E., Hietpas, J., and Palenik, C.S. (*in prep.*). Assessing the potential for adjacent paint layer contribution to the EDS spectra.
- ASTM Guide E-2809 (revision). Although this document is not attributable to any particular author, the PI of this grant provided extensive edits to the revised version of this guide which is currently being rebaloted by OSAC and ASTM.
- Palenik, C.S., Groves, E., Michely, L., Lim, Y.C., and Palenik, S. (2020). A Survey of Elements Detected in Automotive Paint Layers by Scanning Electron Microscope/Energy Dispersive X-Ray Spectrometry (SEM/EDS). AAFS, Anaheim, CA.
- Palenik, C.S., Groves, E., and Palenik, S. (2020). Developments in the Forensic Analysis of Automotive Paints by SEM/EDS. Pittcon Conference, Chicago, IL
- Palenik, C.S. (2019). Development of an objective approach to the characterization and interpretation of paint evidence by SEM/EDS. Forensic Technology Center of Excellence Webinar Series - Emerging Research: Forensic Chemistry.
- Palenik, C.S. and Michely, L. (2018) Analytical considerations for the elemental analysis and forensic comparison of automotive paints. Inter/Micro 2018, Chicago, IL.
- Groves, E.G., Michely, L. and Palenik, C.S. (2018) A Survey of Elements Detected in Multi-layered Automotive Paint Samples by SEM-EDS. Inter/Micro 2018, Chicago, IL.

- Groves, E.G., Michely, L. and Palenik, C.S. (2018) “Examining Elemental Analysis by SEM/EDS in forensic paint comparisons,” Eastern Analytical Symposium. Princeton, NJ.

DISSEMINATION

To date, this work has been presented in at various meetings (see Artifacts section above).

Several publications related to this research are in preparation.

FIGURES

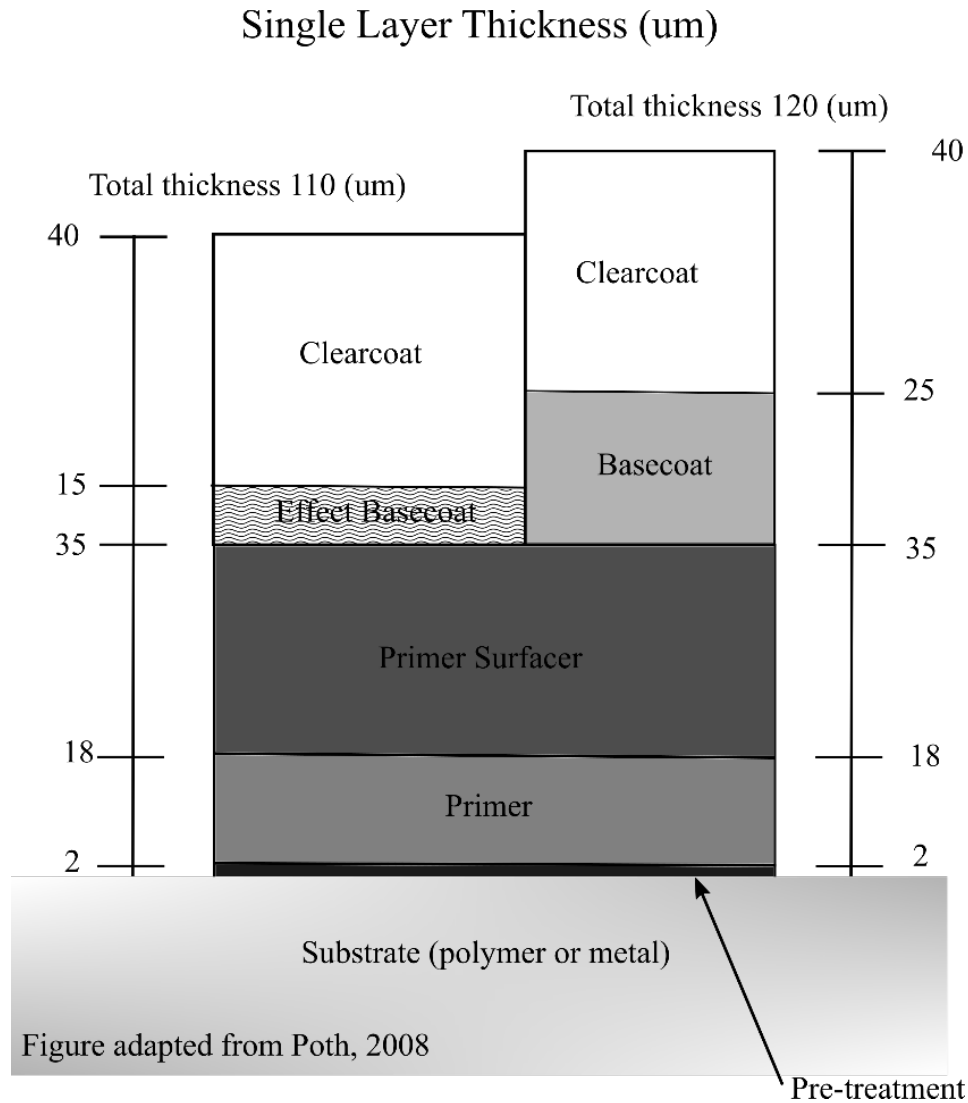
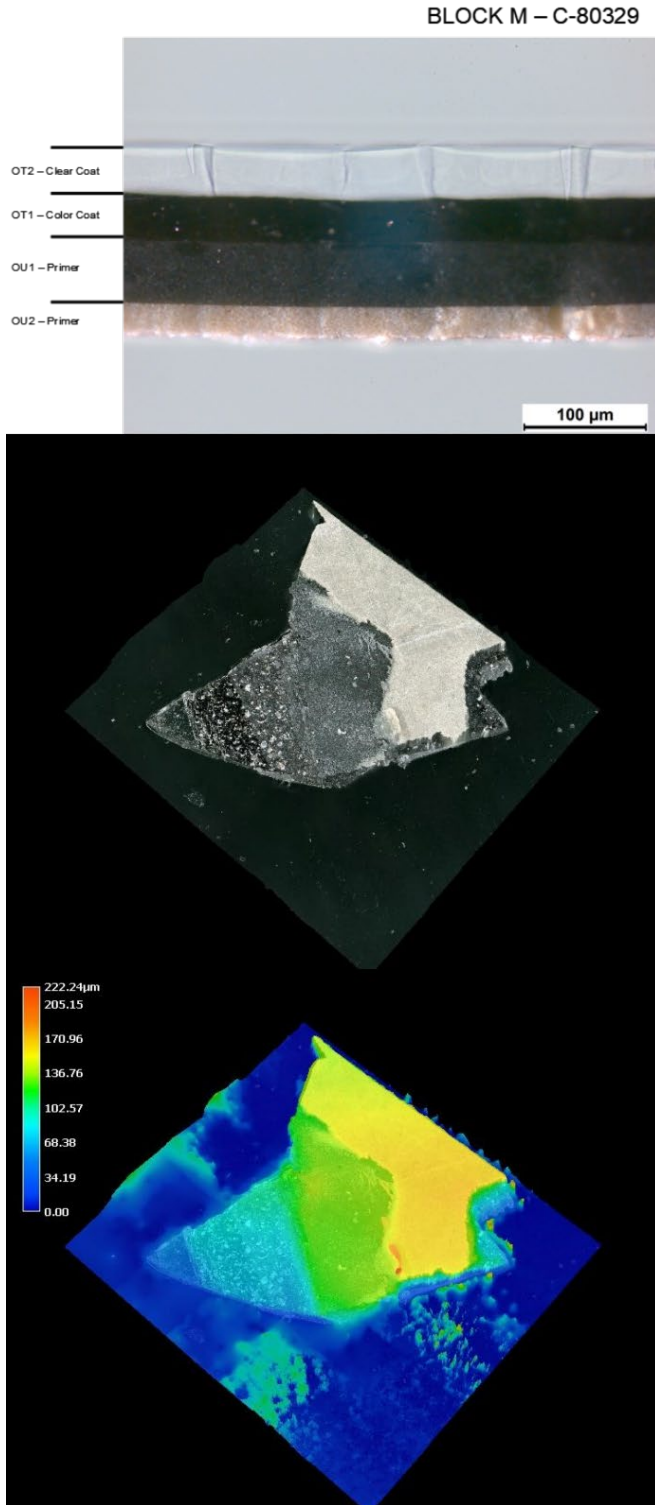


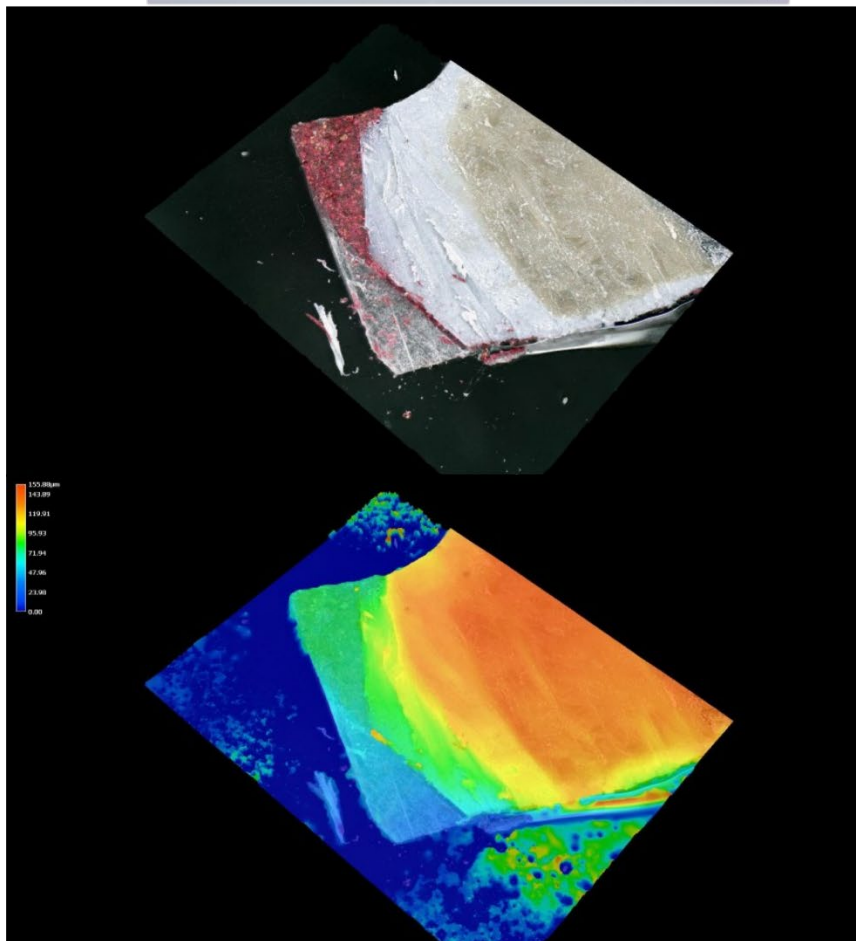
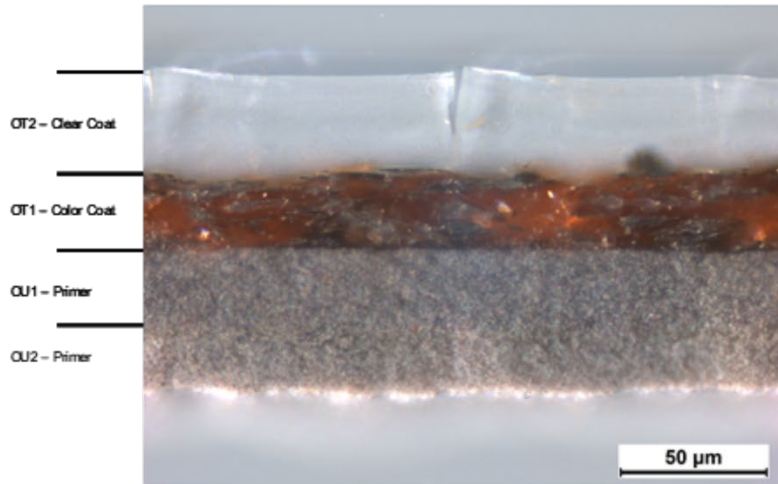
Figure 1. Schematic showing the generalized paint layer structure of modern passenger vehicles.



Microtrace

Figure 2. (top) Thin cross section of a paint chip prepared by microtomy compared to (middle and lower) images of specimens prepared by the “stair-step” method. The middle and lower images show the uneven and irregular topography of the stair-step method by a z-stacking method (middle) and white-light interferometry (lower)..

BLOCK J – C-80313



Microtrace

Figure 3. (top) Thin cross section of a paint chip prepared by microtomy compared to (middle and lower) images of specimens prepared by the “stair-step” method. The middle and lower images show the uneven and irregular topography of the stair-step method by a z-stacking method (middle) and white-light interferometry (lower).

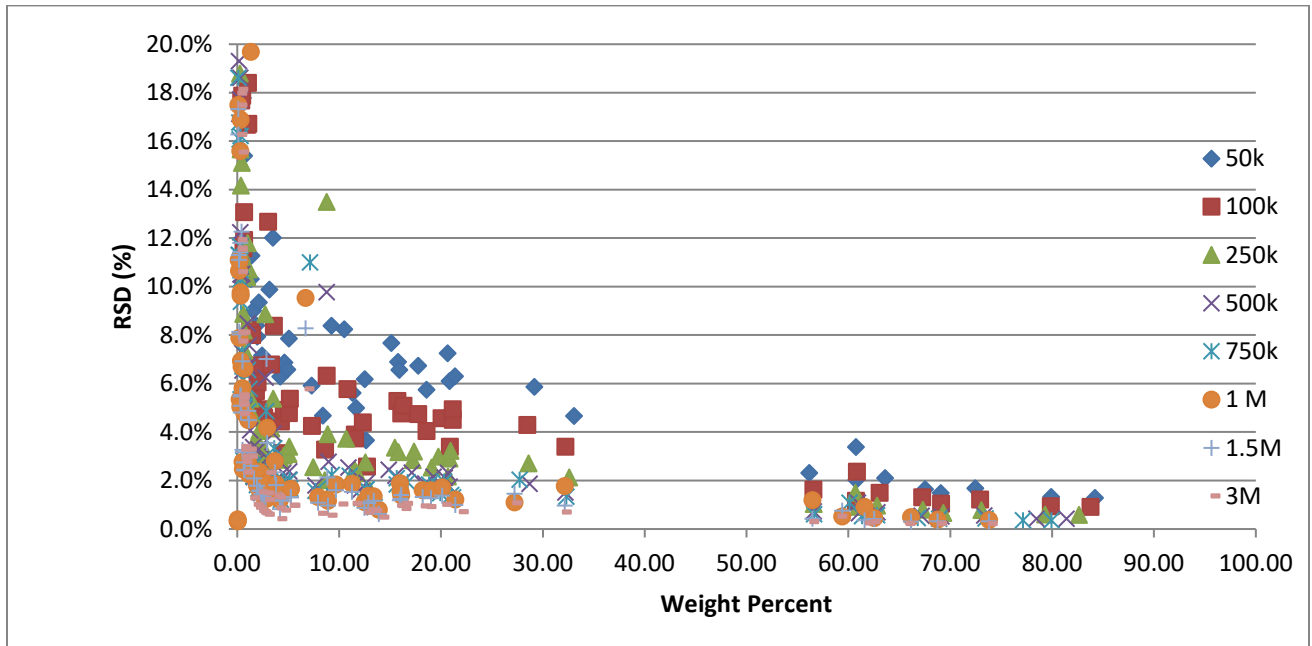


Figure 4. Measurement %RSD vs element wt. % for the eight different total spectrum count criteria.

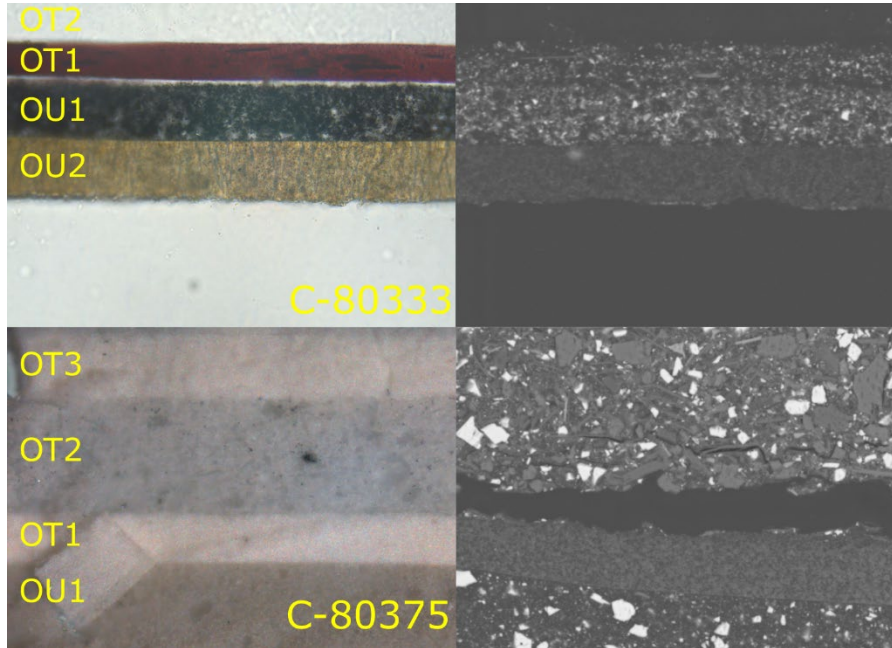


Figure 5. Light and backscattered electron photomicrographs of selected passenger vehicle paint samples. Note the detailed information that can be gained from ultramicrotome sections. OU= original undercoat (primer coats); OT= original topcoat (base and clearcoat).

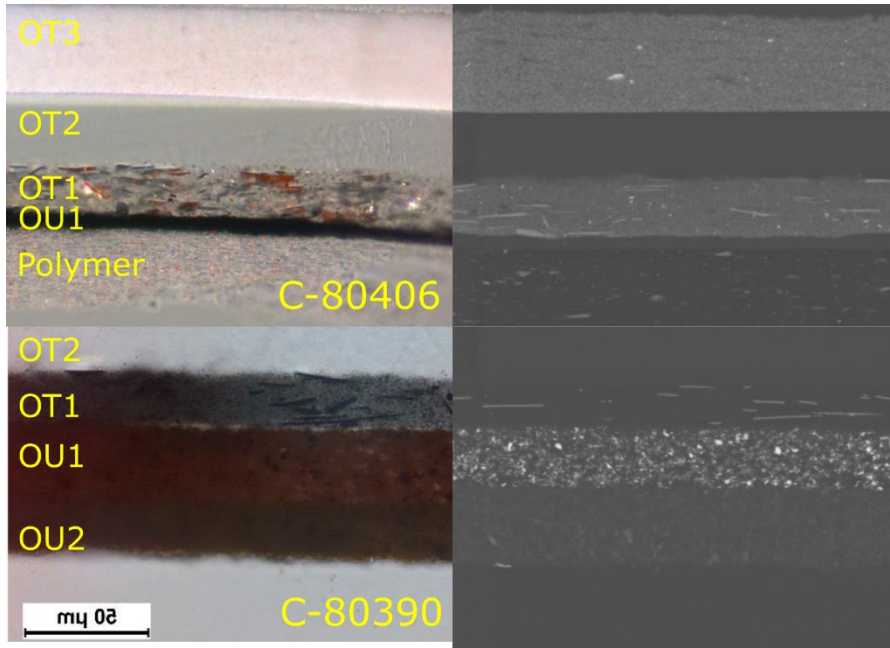


Figure 6. Light and backscattered electron photomicrographs of selected passenger vehicle paint samples.

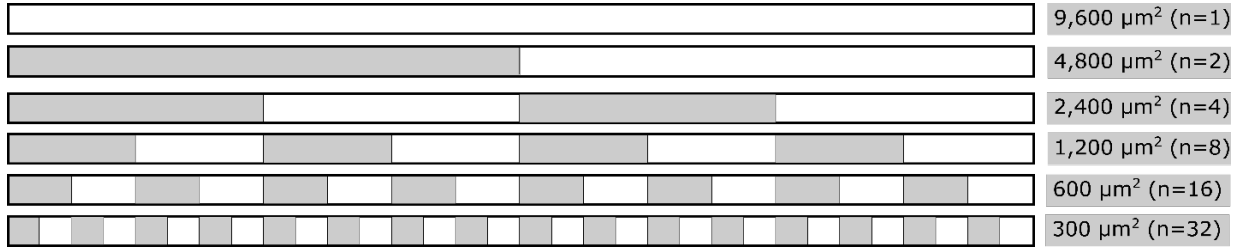


Figure 7. Schematic diagram showing the subdivision sampling scheme for the analyzed paint layers.

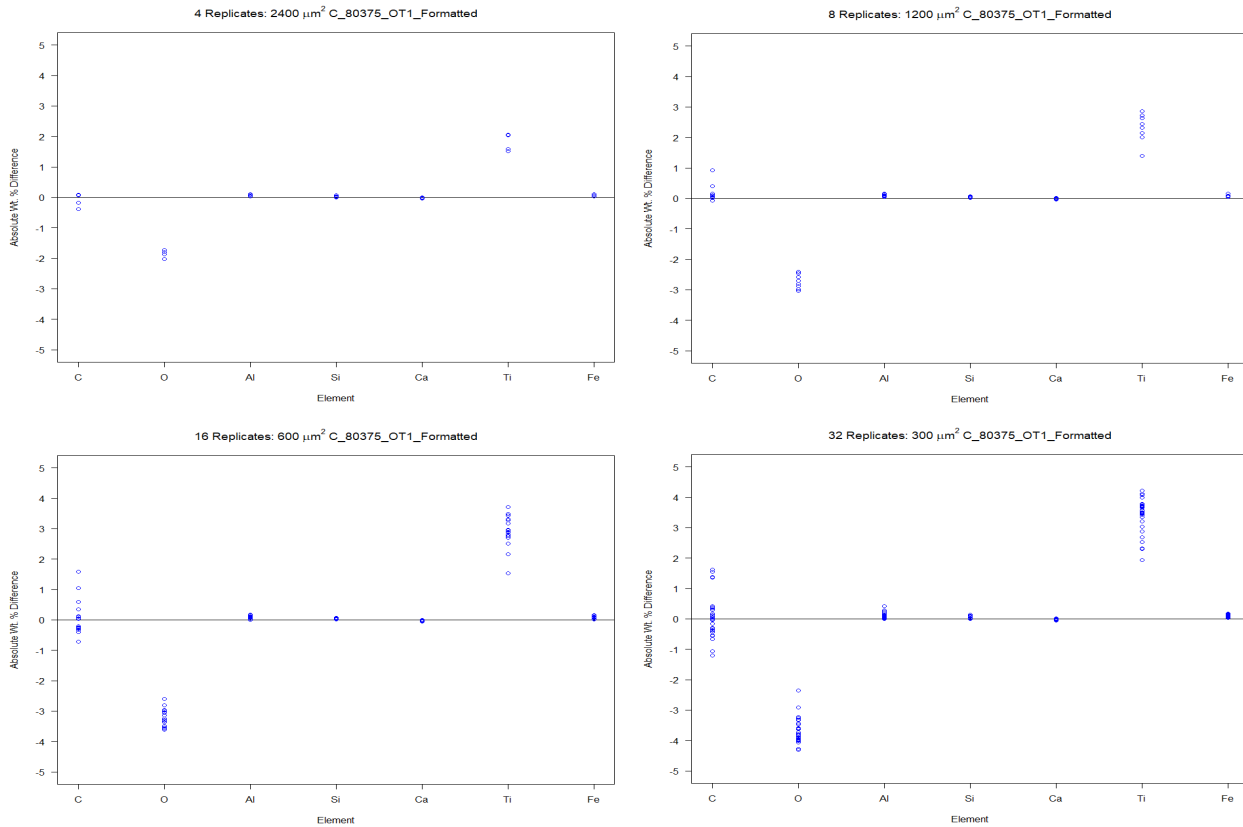


Figure 8. Replicate spectra for different sized analytical areas for sample 80375 OT1 (low).

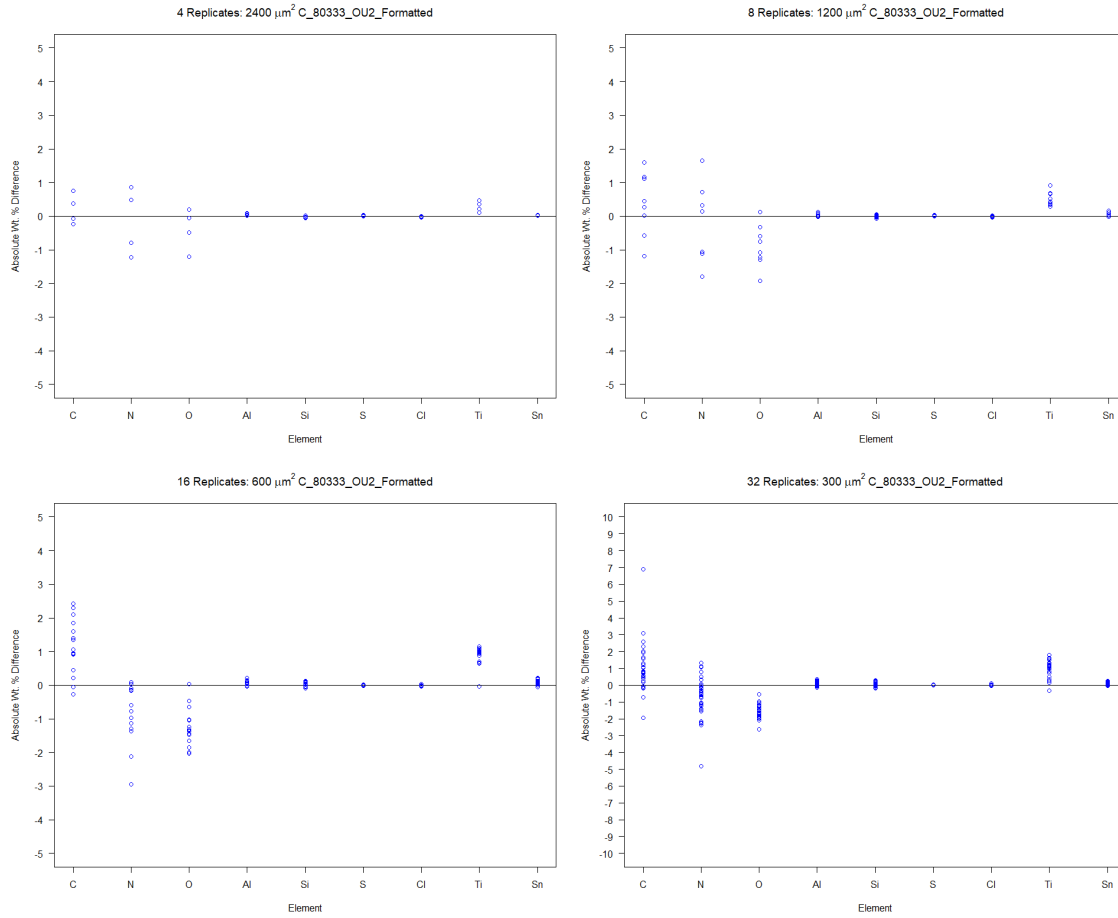


Figure 9. Replicate spectra for different sized analytical areas for sample 80333 OU2 (low).

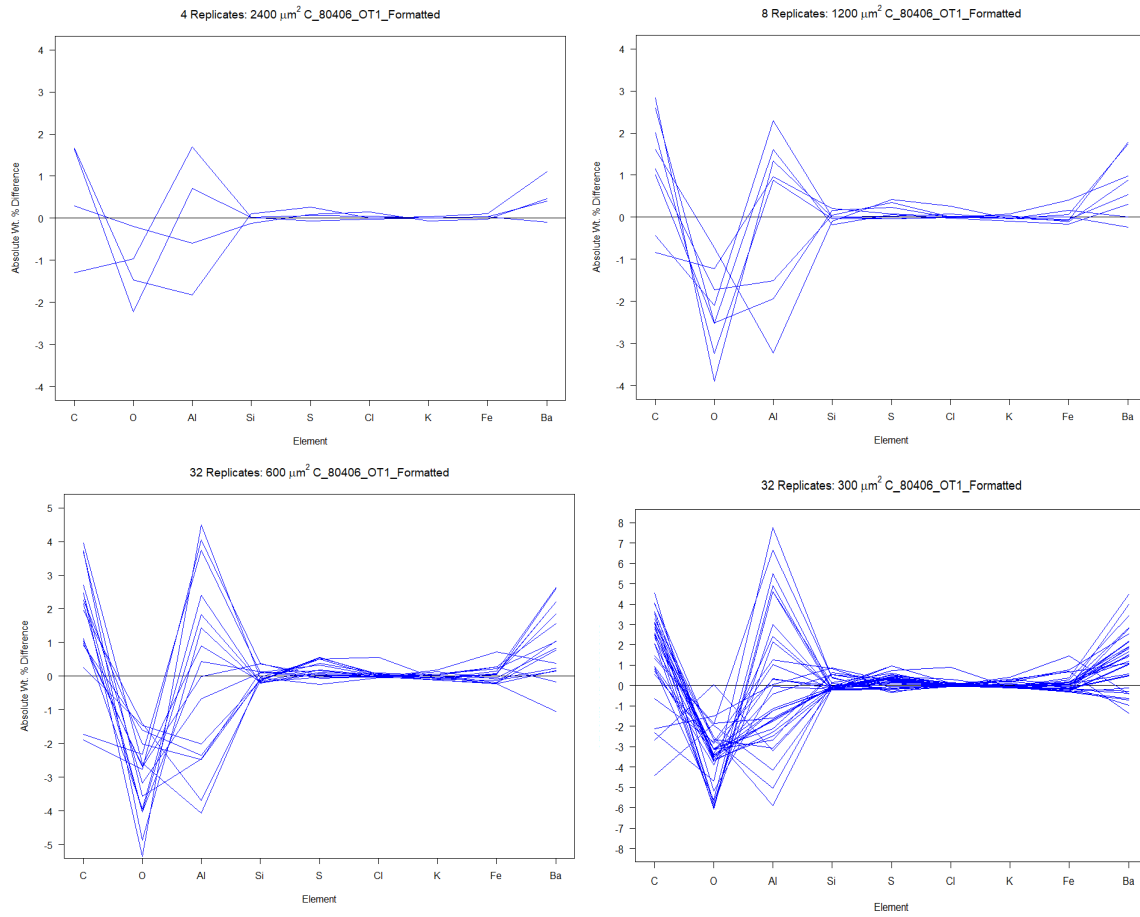


Figure 10. Replicate spectra for different sized analytical areas for sample 80406 OT1 (medium).

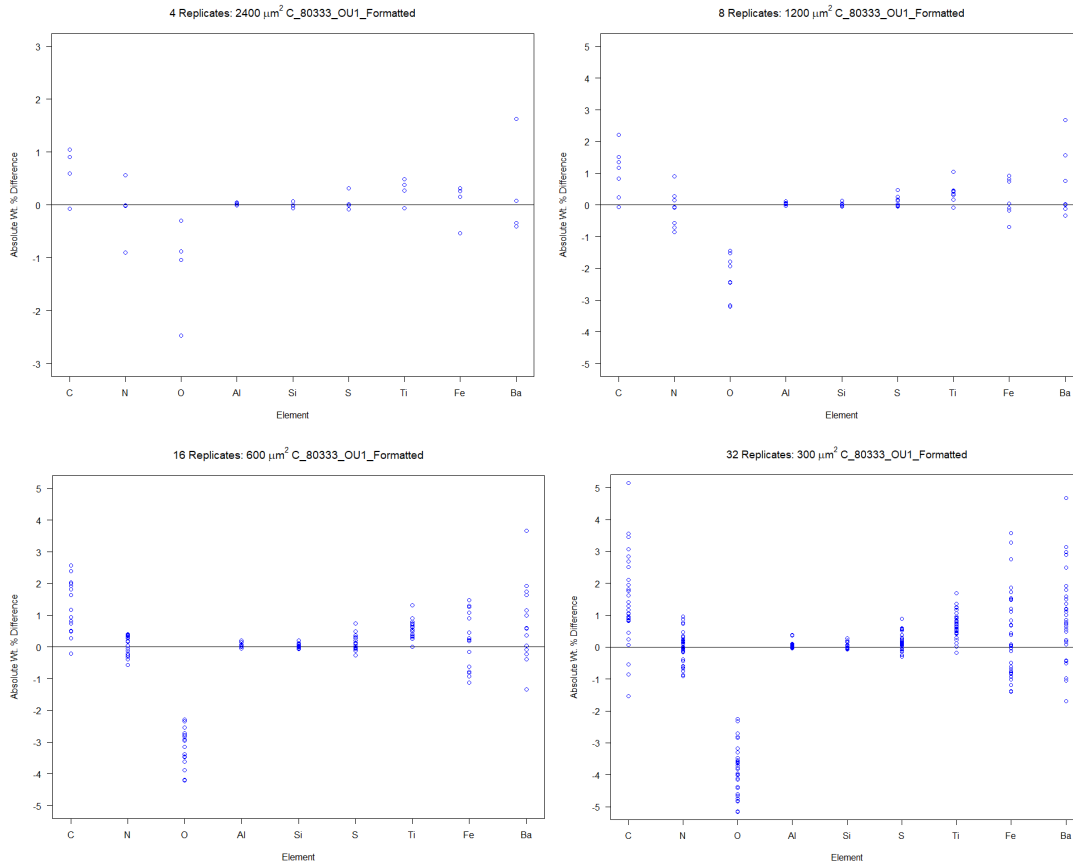


Figure 11. Replicate spectra for different sized analytical areas for sample 80333 OUI (medium).

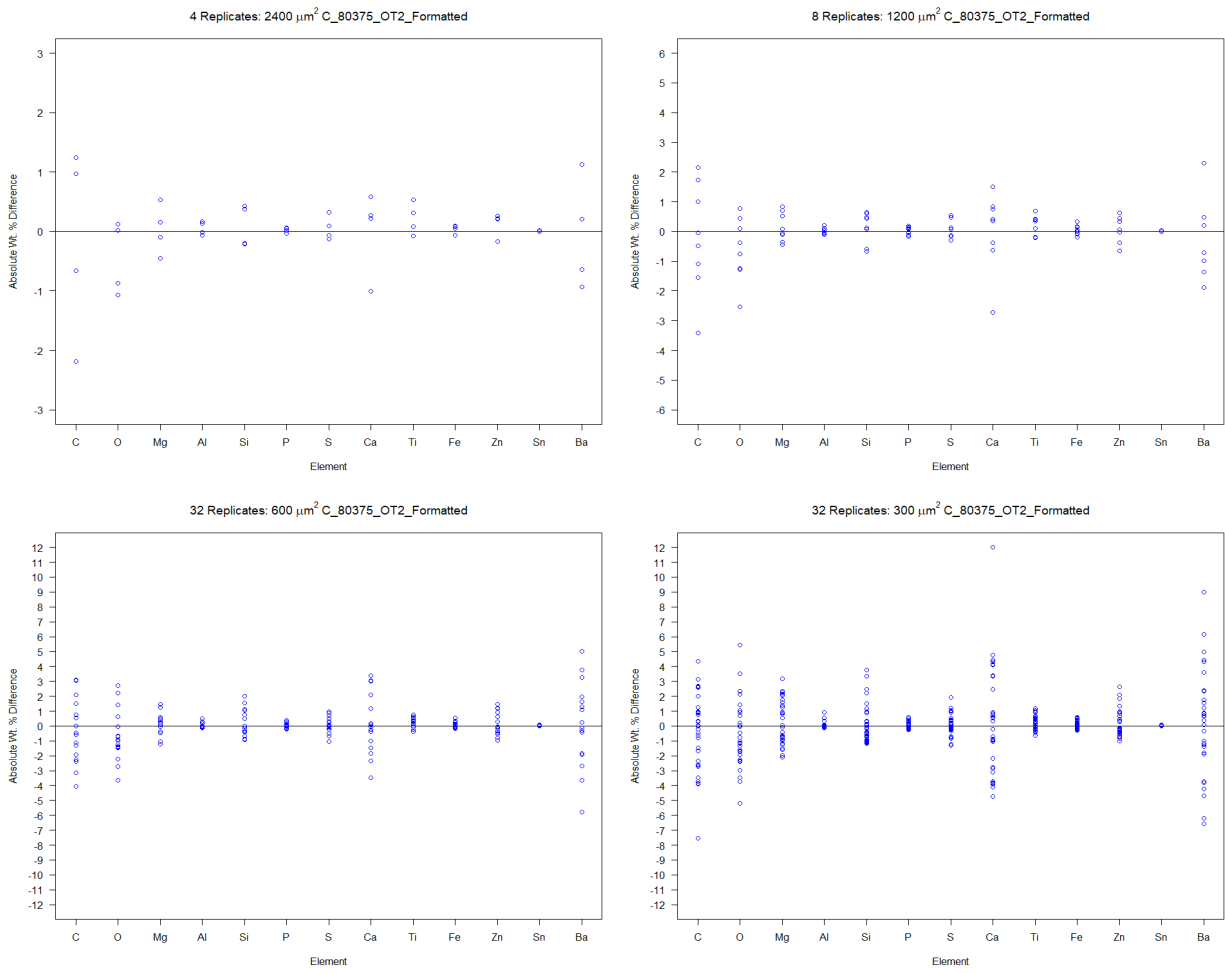


Figure 12. Replicate spectra for different sized analytical areas for sample 80375 OT2 (high).

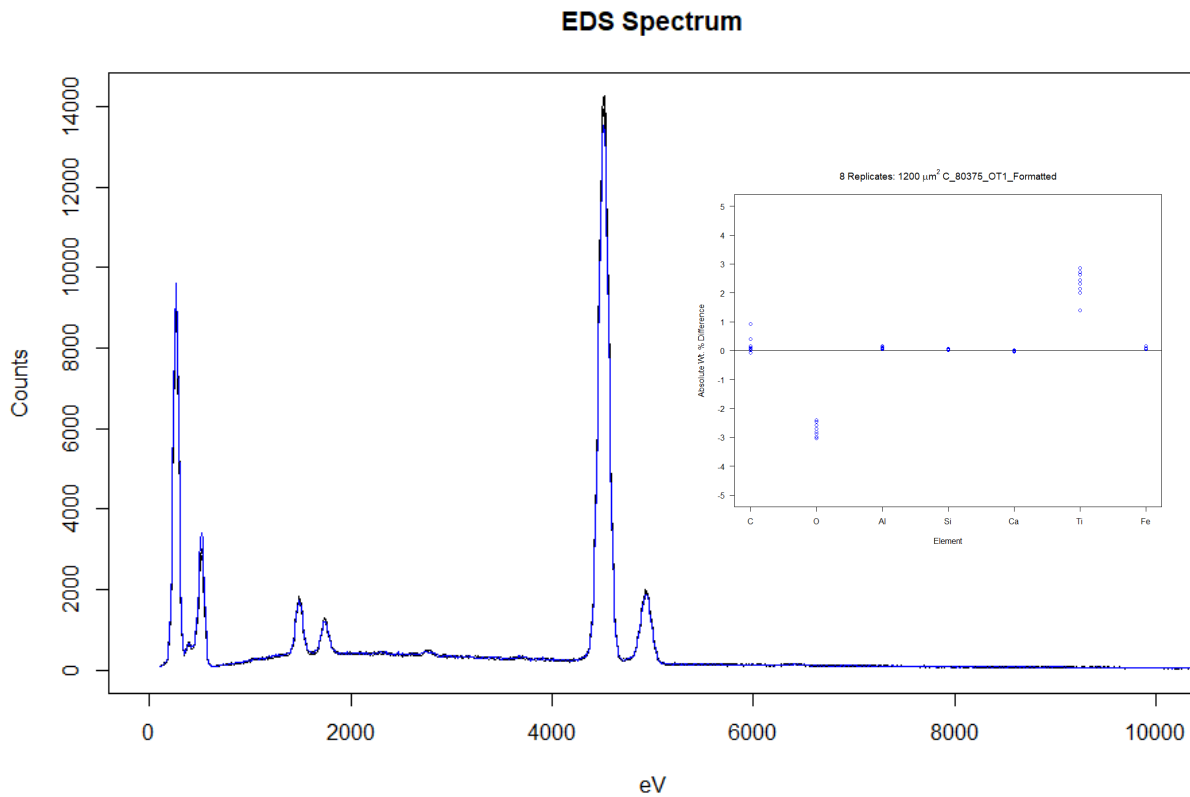


Figure 13. Observed variability in layer 80375 OT1 (low) in spectral space and wt. % values for the 8 replicate spectra collected from 1200 μm². The parent spectrum (collected from 9600 μm²) is shown in blue. The two spectra shown in black represent the 2.5 and 97.5 percentiles.

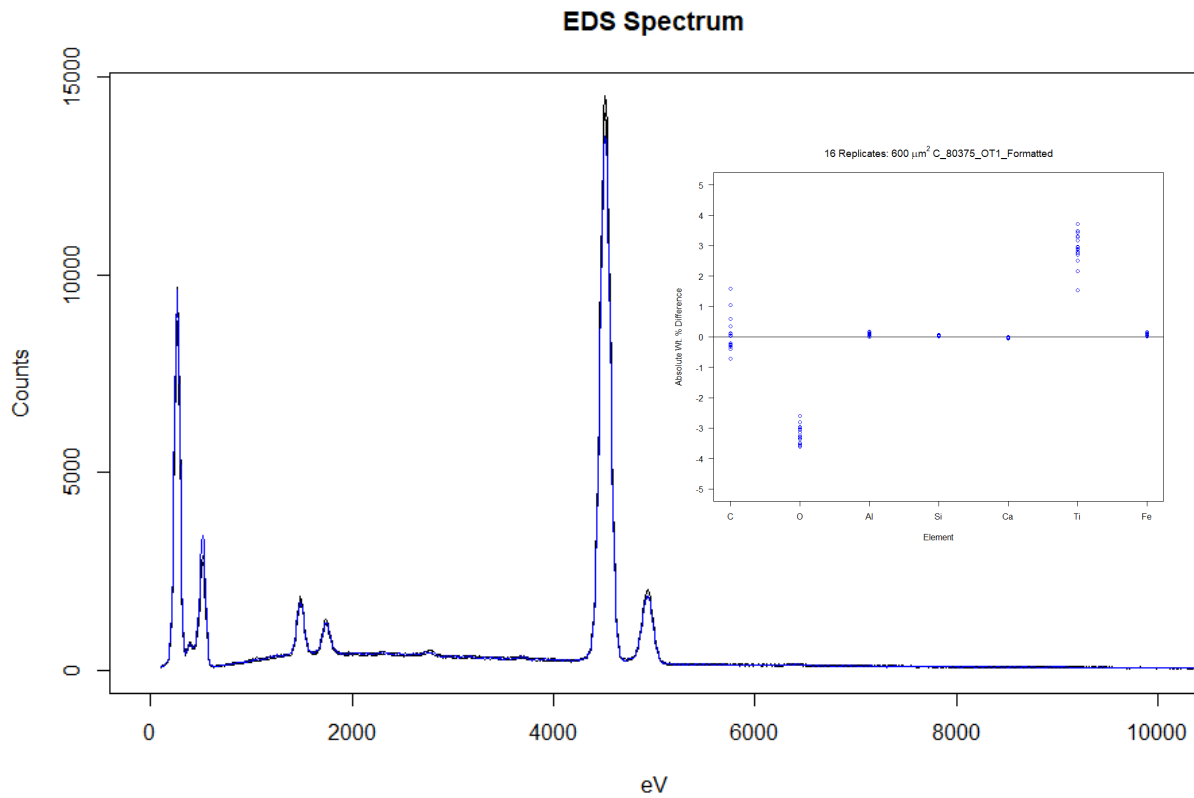


Figure 14. Observed variability in layer 80375 OT1 (low) in spectral space and wt. % values for the 16 replicated spectra collected from 600 μm². The parent spectrum (9600 μm²) is shown in blue. The two spectra shown in black represent the 2.5 and 97.5 percentiles.

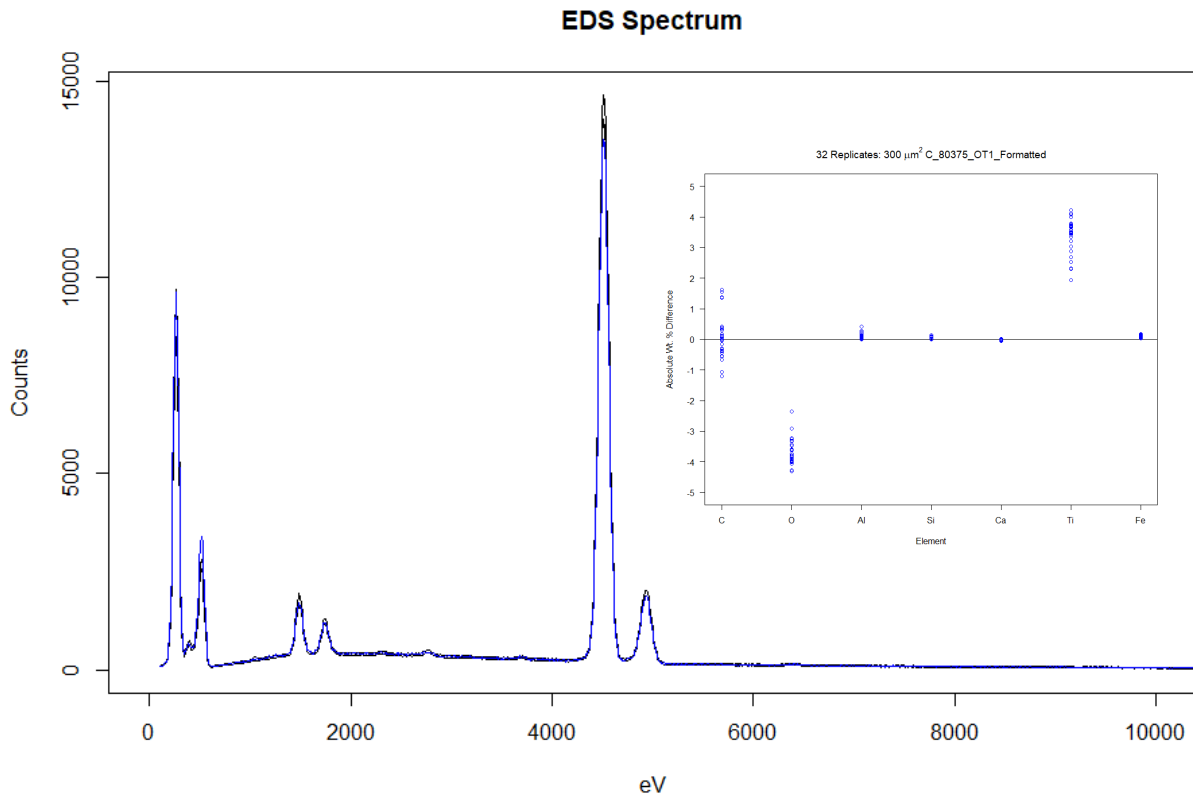


Figure 15. Observed variability in layer 80375 OT1 (low) in spectral space and wt. % values for the 32 replicated spectra collected from 1200 μm². The parent spectrum (collected from 9600 μm²) is shown in blue. The two spectra shown in black represent the 2.5 and 97.5 percentiles.

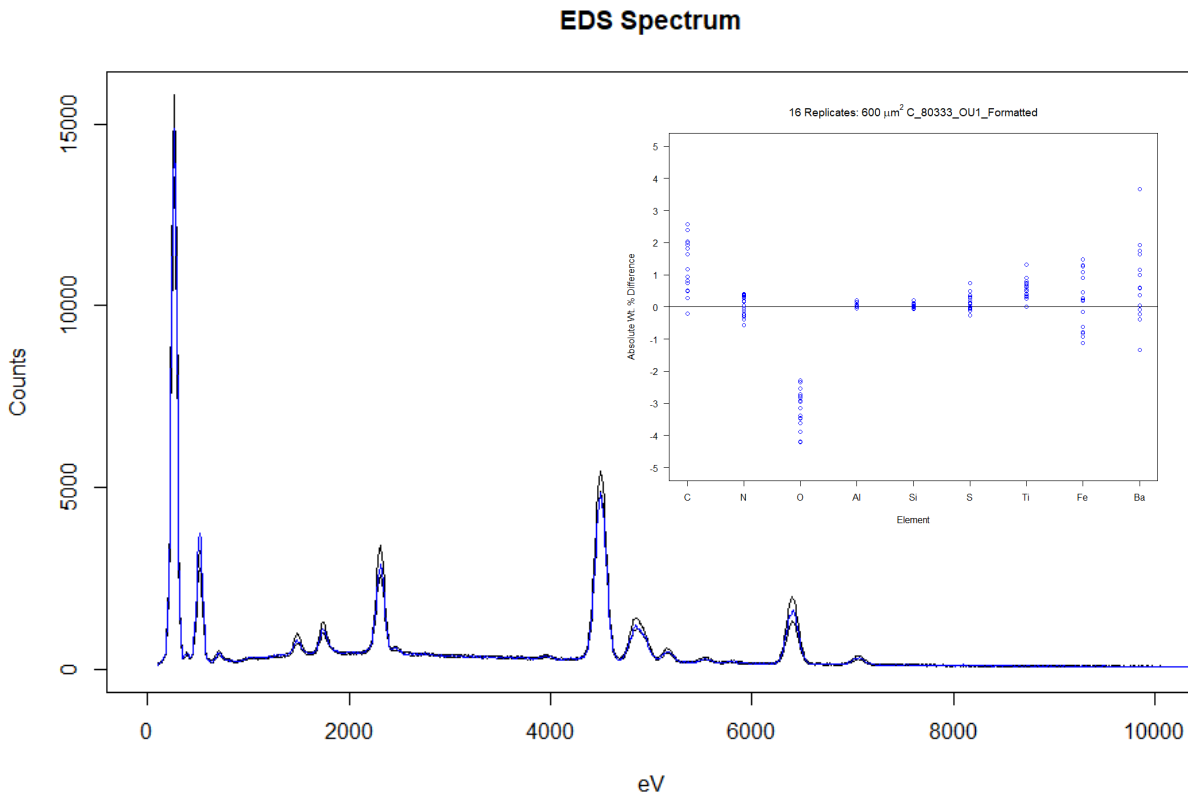


Figure 16. Observed variability in layer 80333 OU1 (medium) in spectral space and wt. % values for the 16 replicated spectra collected from 600 μm^2 . The parent spectrum (collected from 9600 μm^2) is shown in blue. The two spectra shown in black represent the 2.5 and 97.5 percentiles.

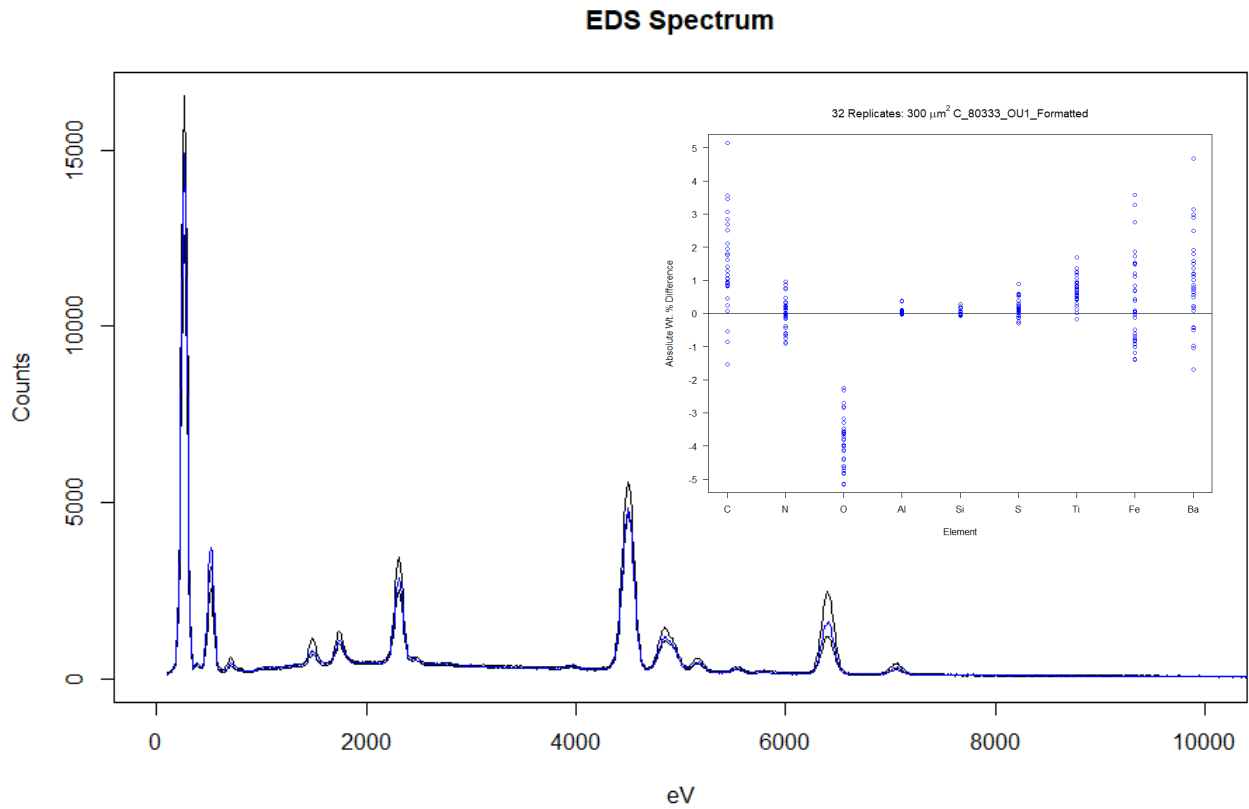
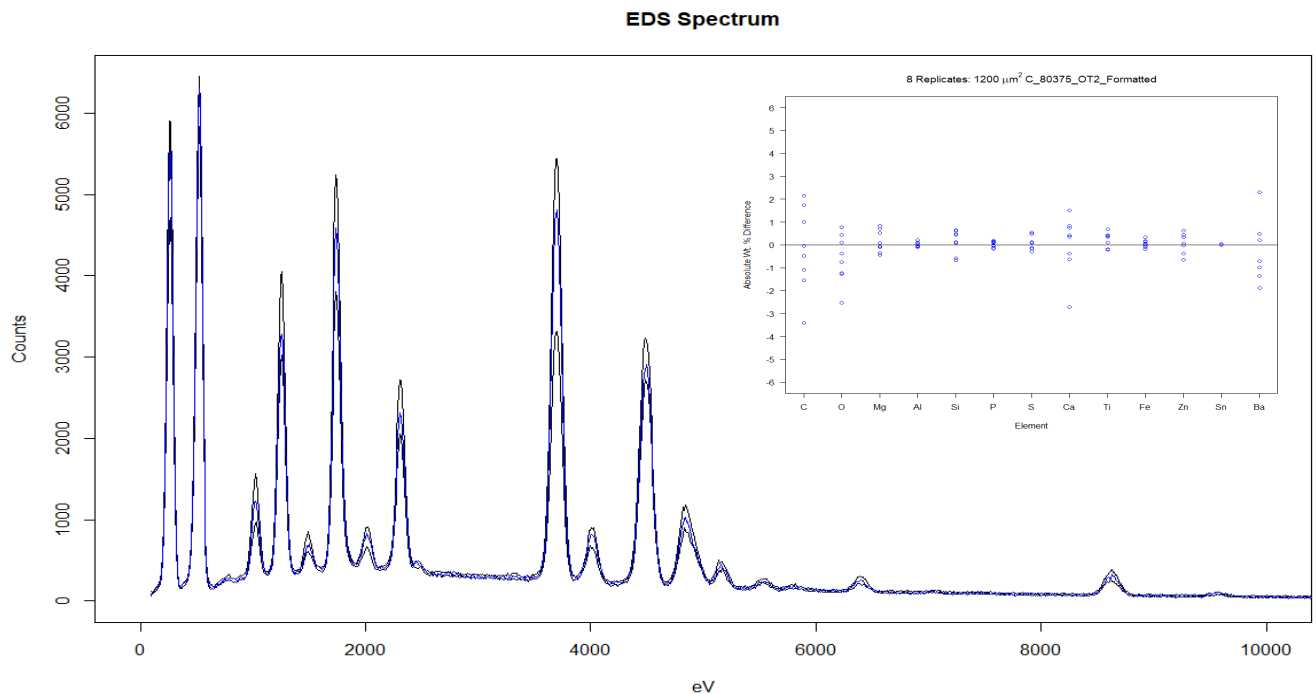
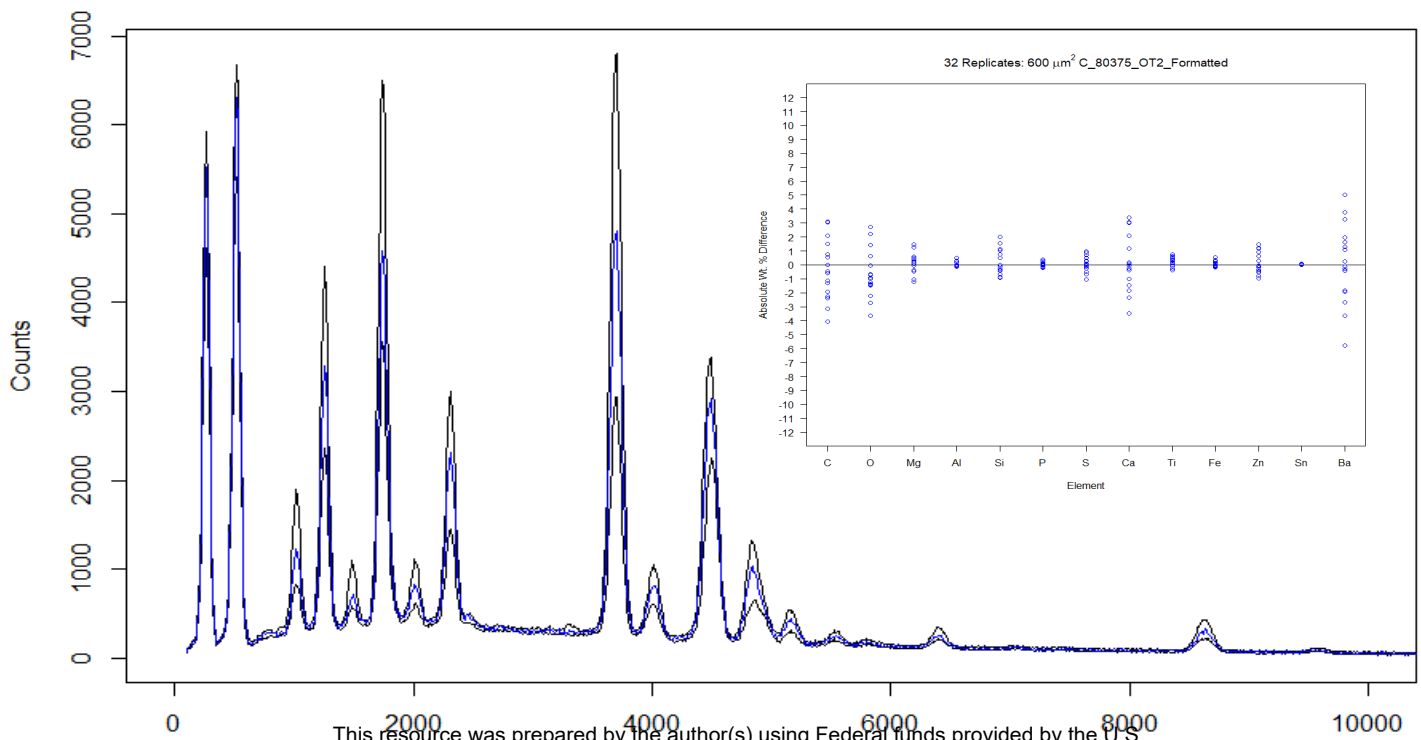


Figure 17. Observed variability in layer 80333 OU1 (medium) in spectral space and wt. % values for the 32 replicated spectra collected from 300 μm². The parent spectrum (9600 μm²) is shown in blue. The two spectra shown in black represent the replicates.



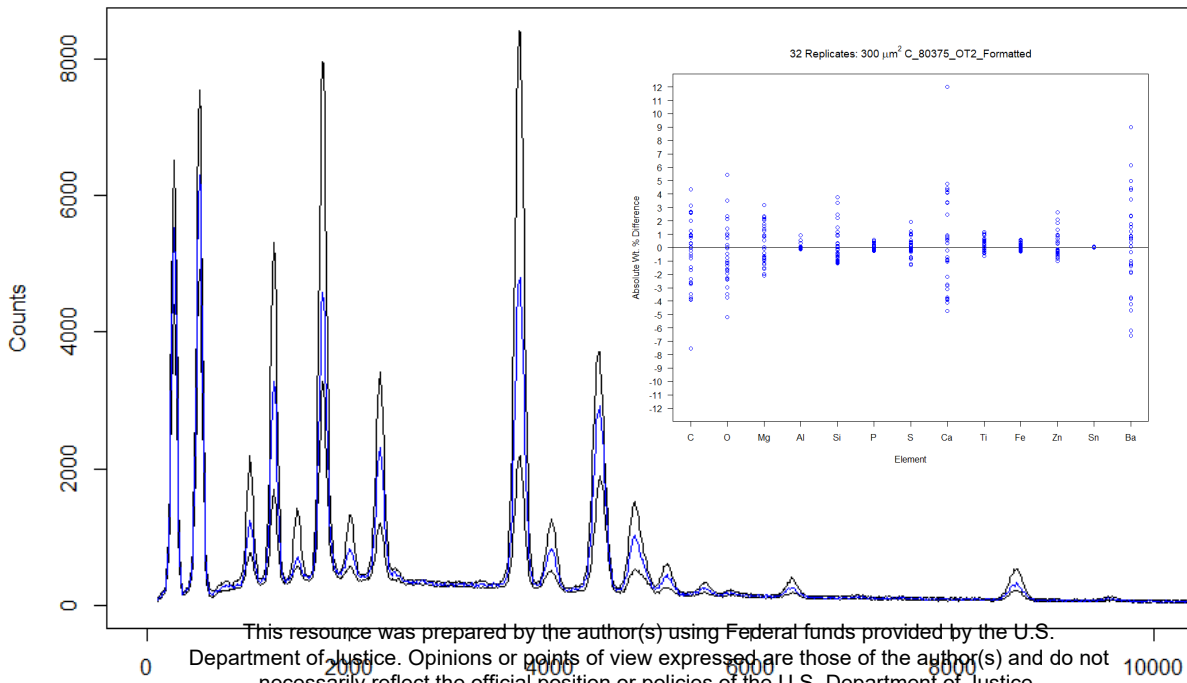
Microtrace

EDS Spectrum



This resource was prepared by the author(s) using Federal funds provided by the U.S. Department of Justice. Opinions or points of view expressed are those of the author(s) and do not necessarily reflect the official position or policies of the U.S. Department of Justice.

EDS Spectrum



This resource was prepared by the author(s) using Federal funds provided by the U.S. Department of Justice. Opinions or points of view expressed are those of the author(s) and do not necessarily reflect the official position or policies of the U.S. Department of Justice.

Figure 20. Observed variability in layer 80375 OT2 (high) in spectral space and wt. % values for the 32 replicated spectra collected from 300 μm^2 . The parent spectrum (collected from 9600 μm^2) is shown in blue. The two spectra shown in black represent the 2.5 and 97.5 percentiles.

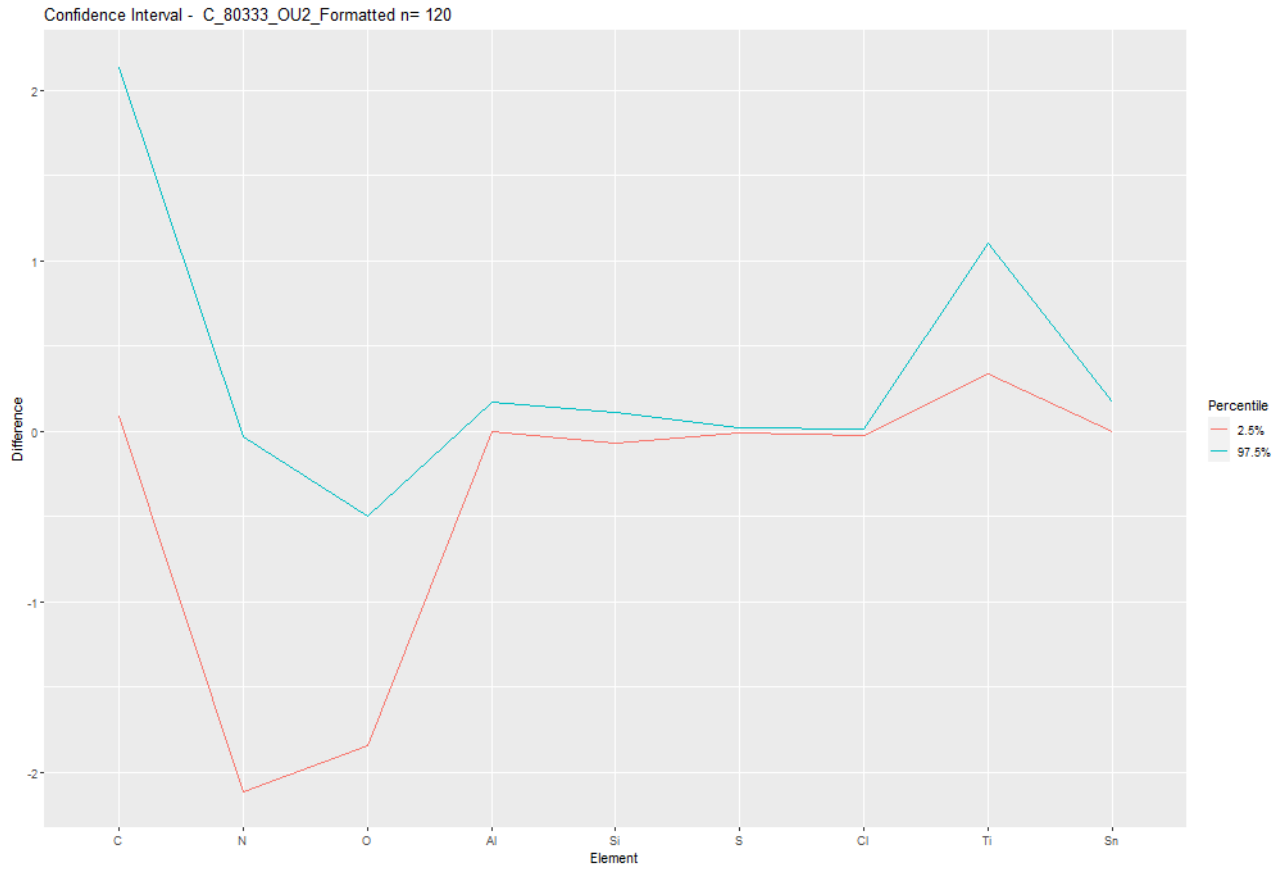


Figure 21. Paint layer 80333 OU2, low degree of heterogeneity. The 95% data window for all 120 combinations of two 600 μm² spectra.



Figure 22. Paint layer 80333 OU2, low degree of heterogeneity. The 95% data window for all 35960 combinations of four 300 μm^2 spectra.

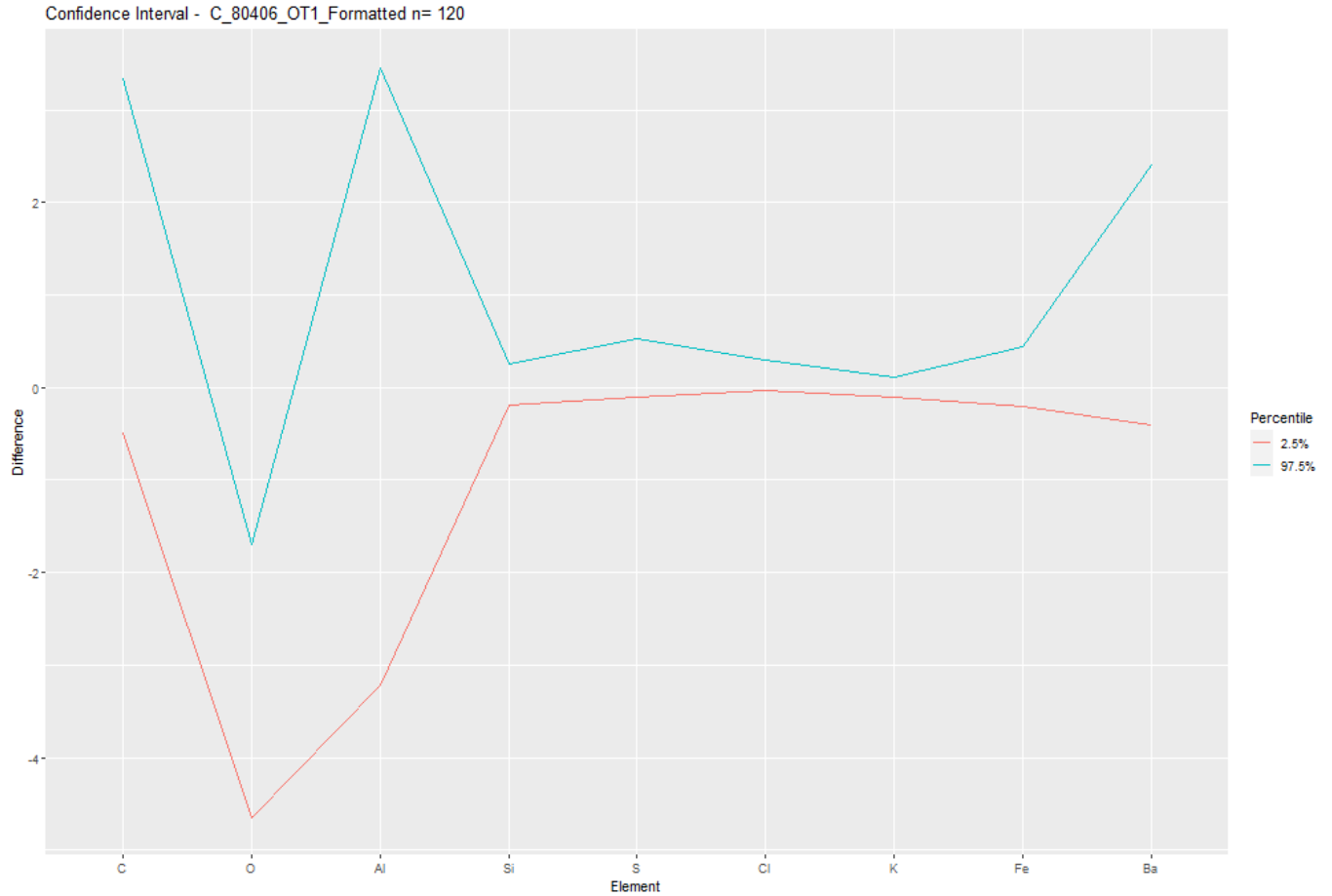


Figure 23. Paint layer 80406 OT1, medium degree of heterogeneity. The 95% data window for all 120 combinations of two 600 μm^2 spectra.

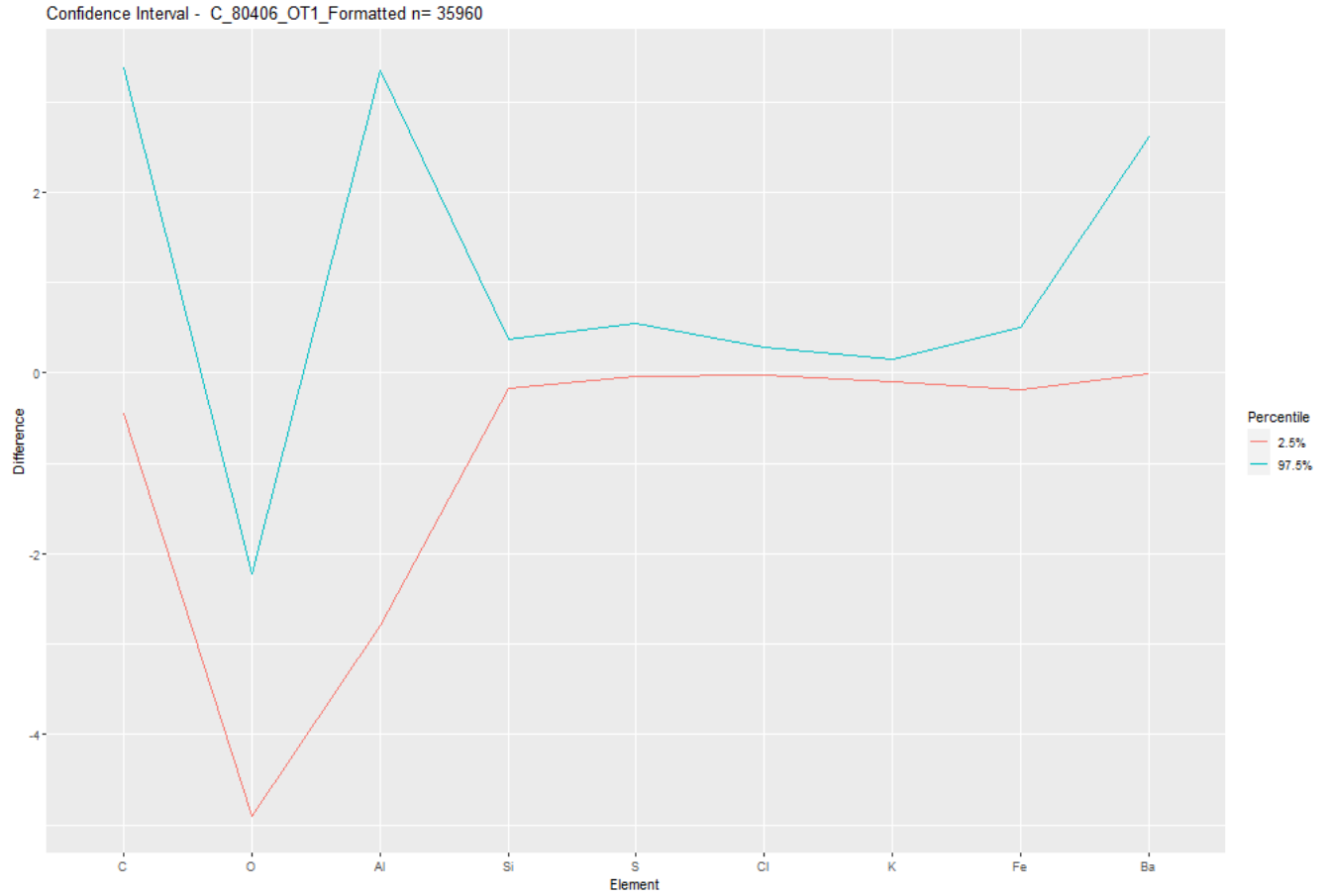


Figure 24. Paint layer 80406 OT1, medium degree of heterogeneity. The 95% data window for all 35960 combinations of four 300 μm^2 spectra.

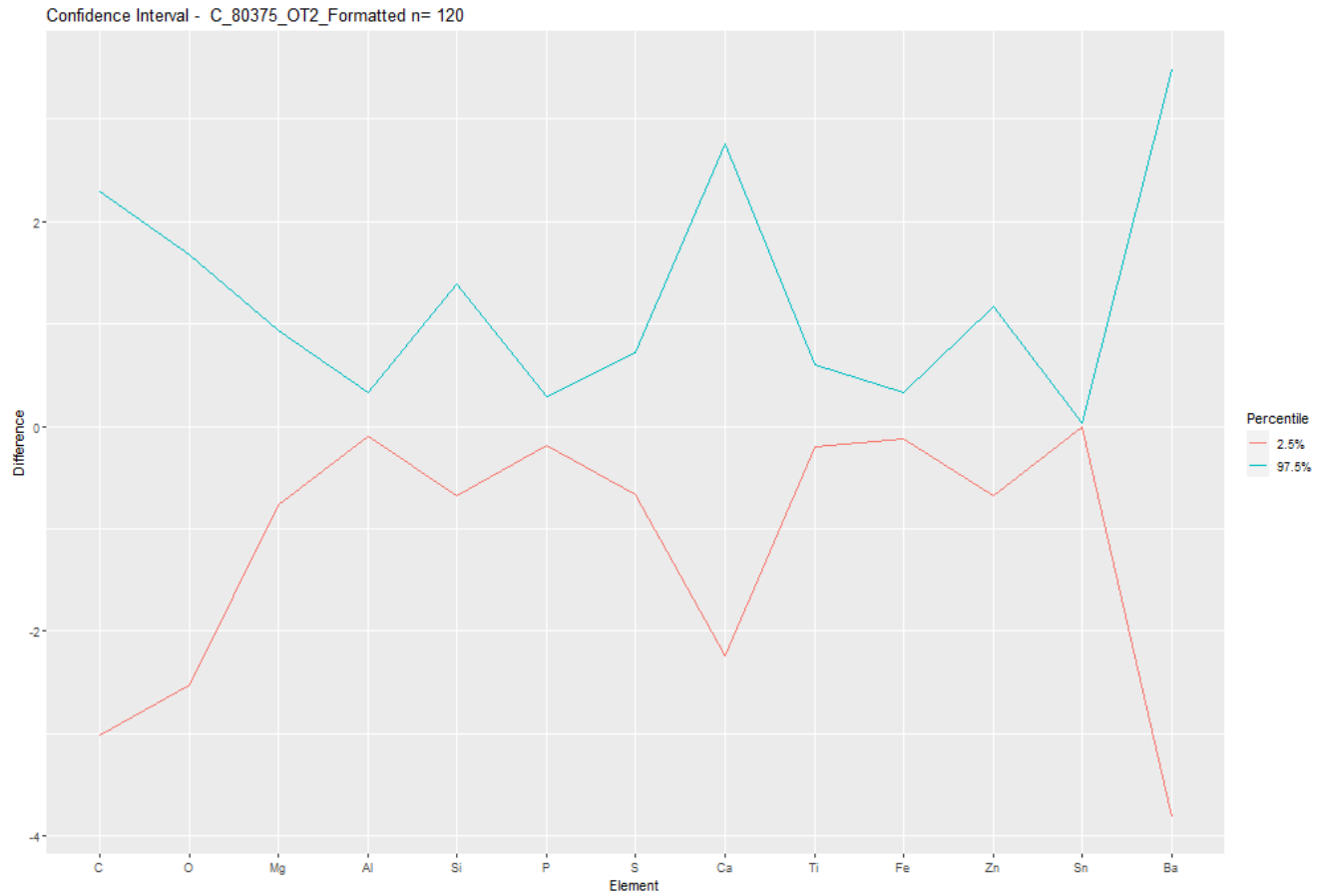


Figure 25. Paint layer 80375 OT2, high degree of heterogeneity. The 95% data window for all 120 combinations of two 600 μm^2 spectra.

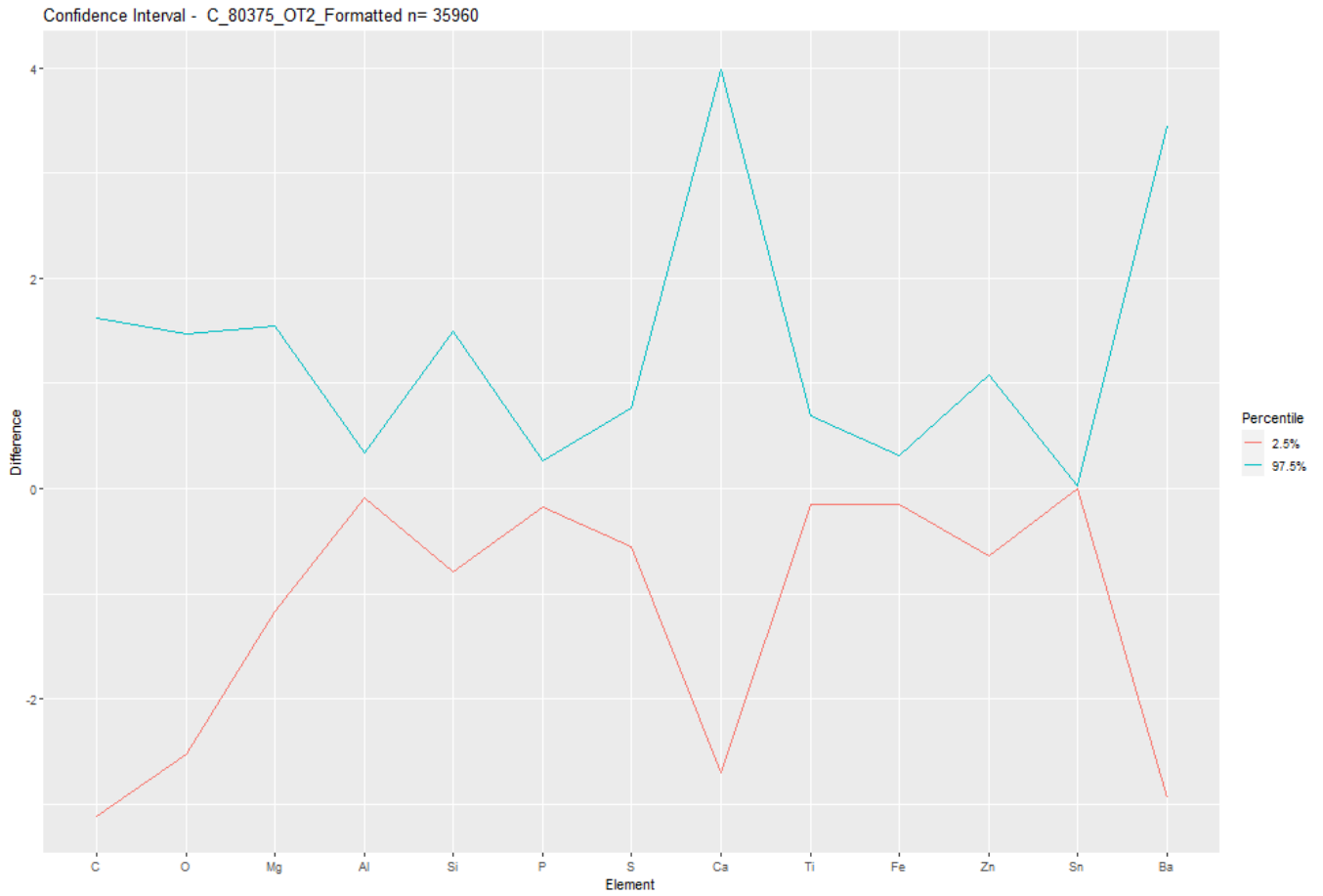


Figure 26. Paint layer 80375 OT2, high degree of heterogeneity. The 95% data window for all 35960 combinations of four 300 μm^2 spectra.

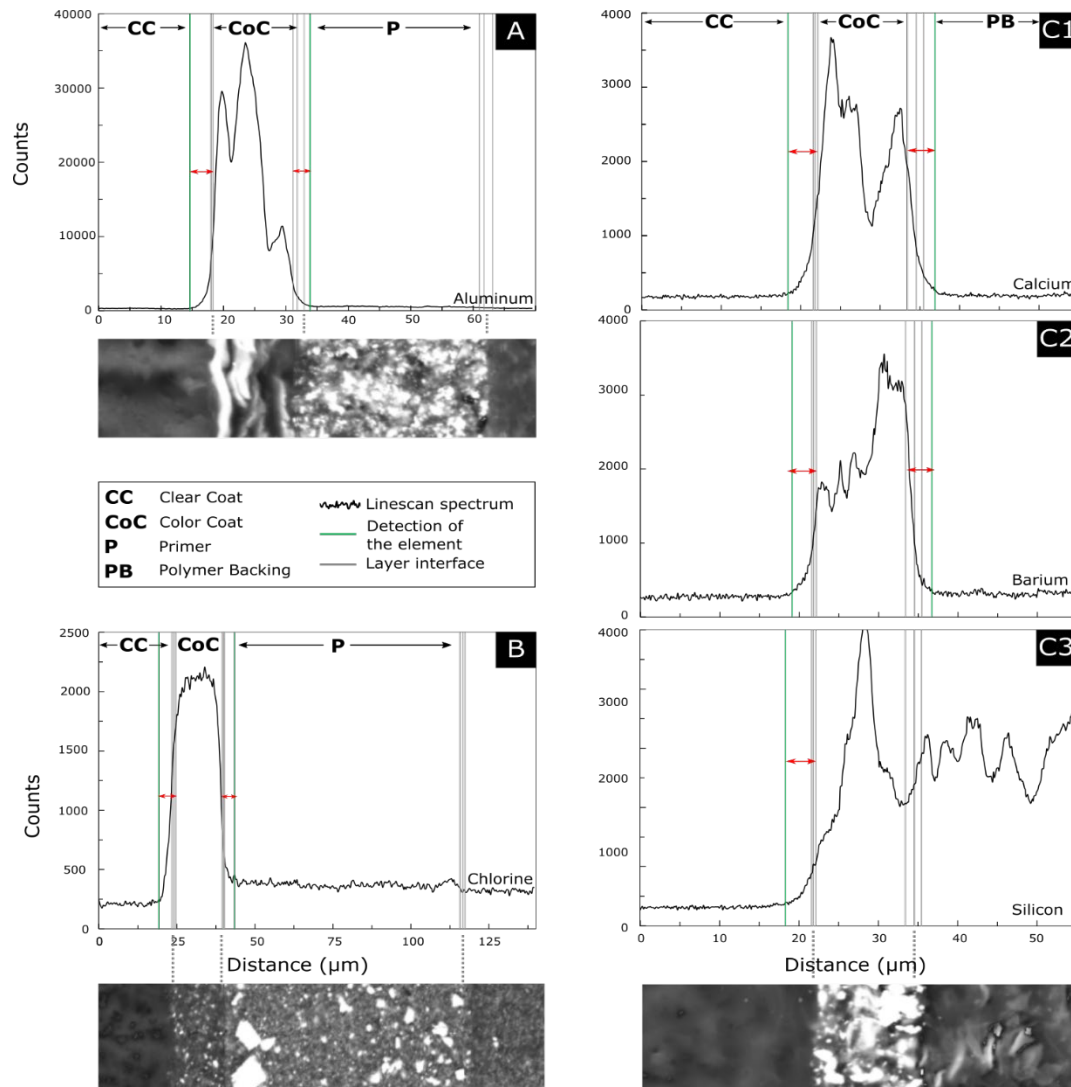


Figure 27. Graphs display measured counts extracted from line scans of a selection of samples and elements as a function of distance (starting point of the line scan in the Clear Coat = 0 μm). Grey lines reflect the variation in the distance from a layer interface to the starting point of the line scan, while green lines represent from which point onwards an elemental signal from the adjacent layer can be detected. A) Sample AZ-80467 B) Sample O-80351 C) Sample-80068.

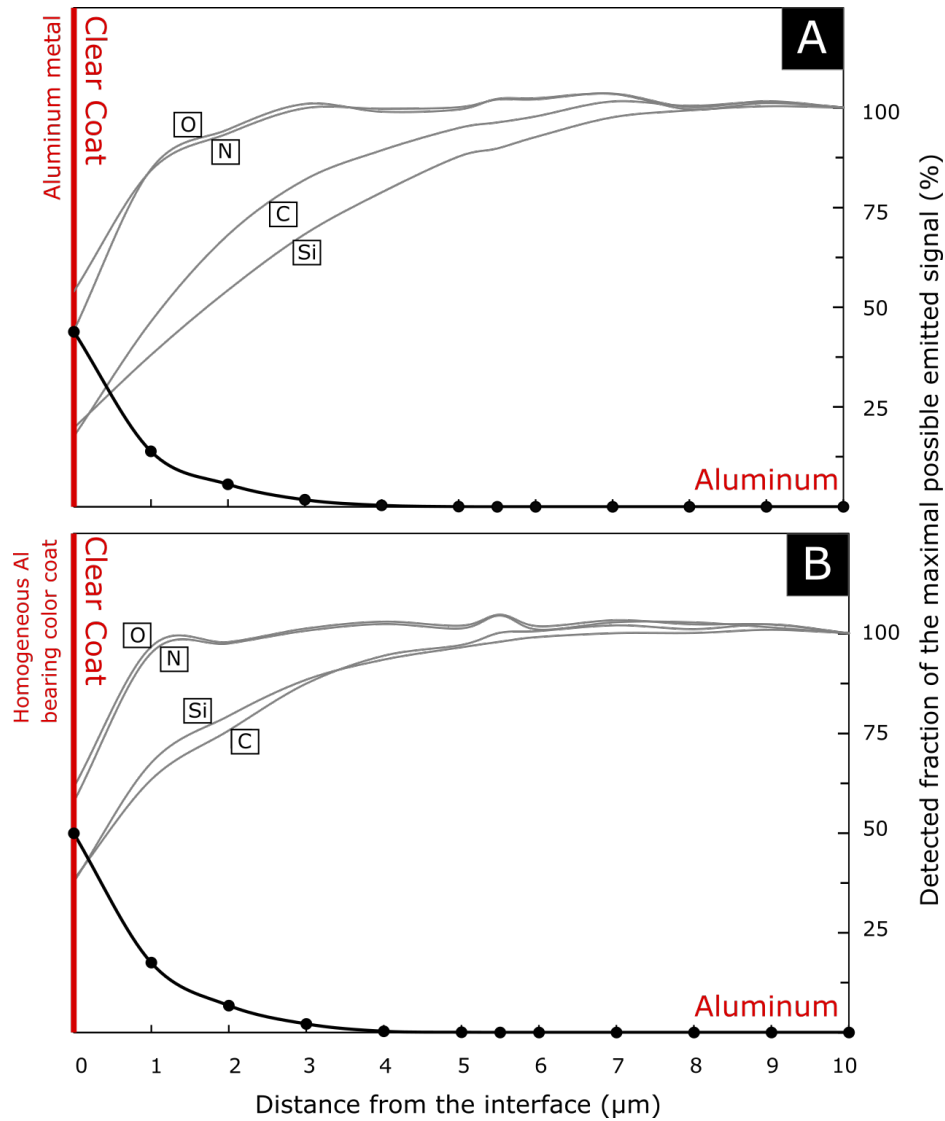


Figure 28: Monte Carlo simulation of emitted X-rays of a beam targeted onto a basic clear coat close to the interface of A) Aluminum metal and B) a homogeneous aluminum bearing color coat. The contribution of aluminum X-rays measured in the clear coat as a function of distance (10-0 μm) to the interface is displayed as the fraction of the maximal possible emitted X-ray signal in %. Variations in the emitted signal of C, N, O and Si are similarly displayed.

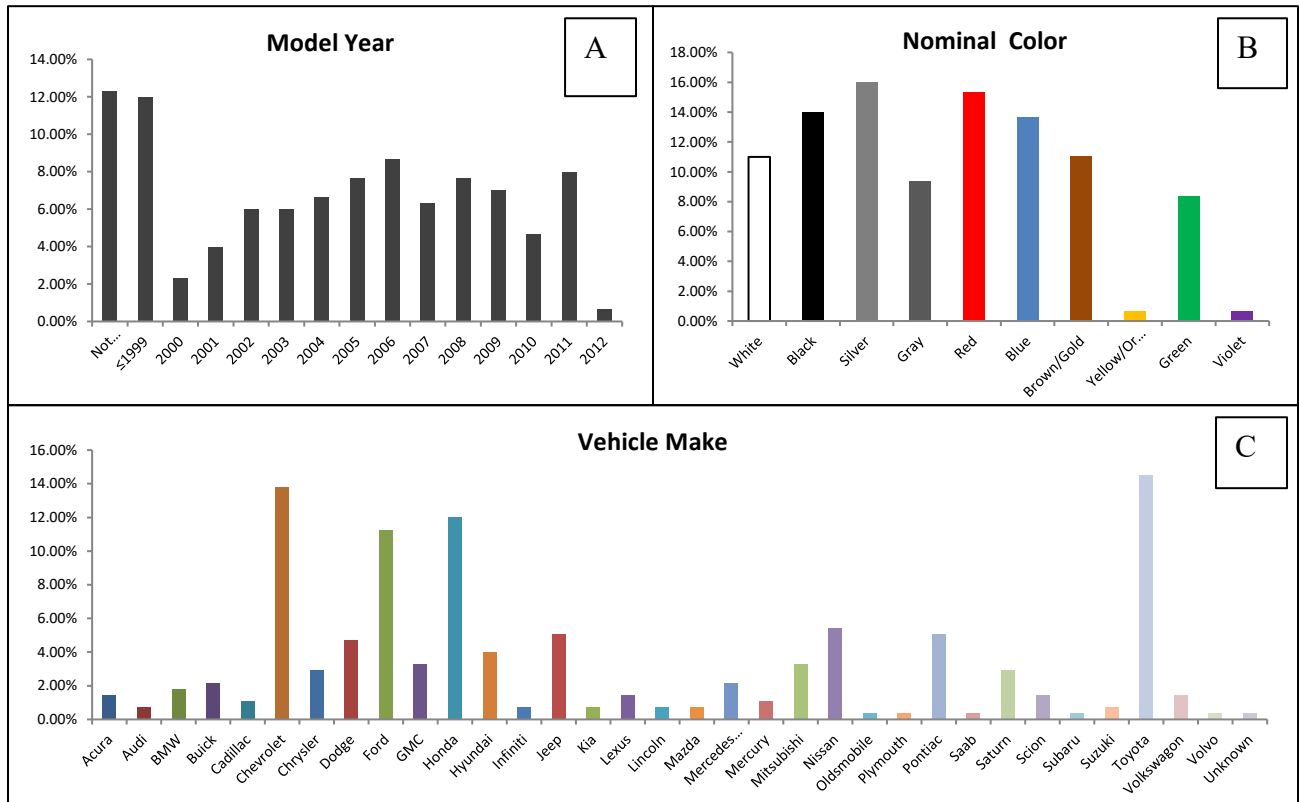


Figure 29 Distribution of automotive samples (n=300) in the surveyed population by (A) model year, (B) nominal color, and (C) vehicle make.

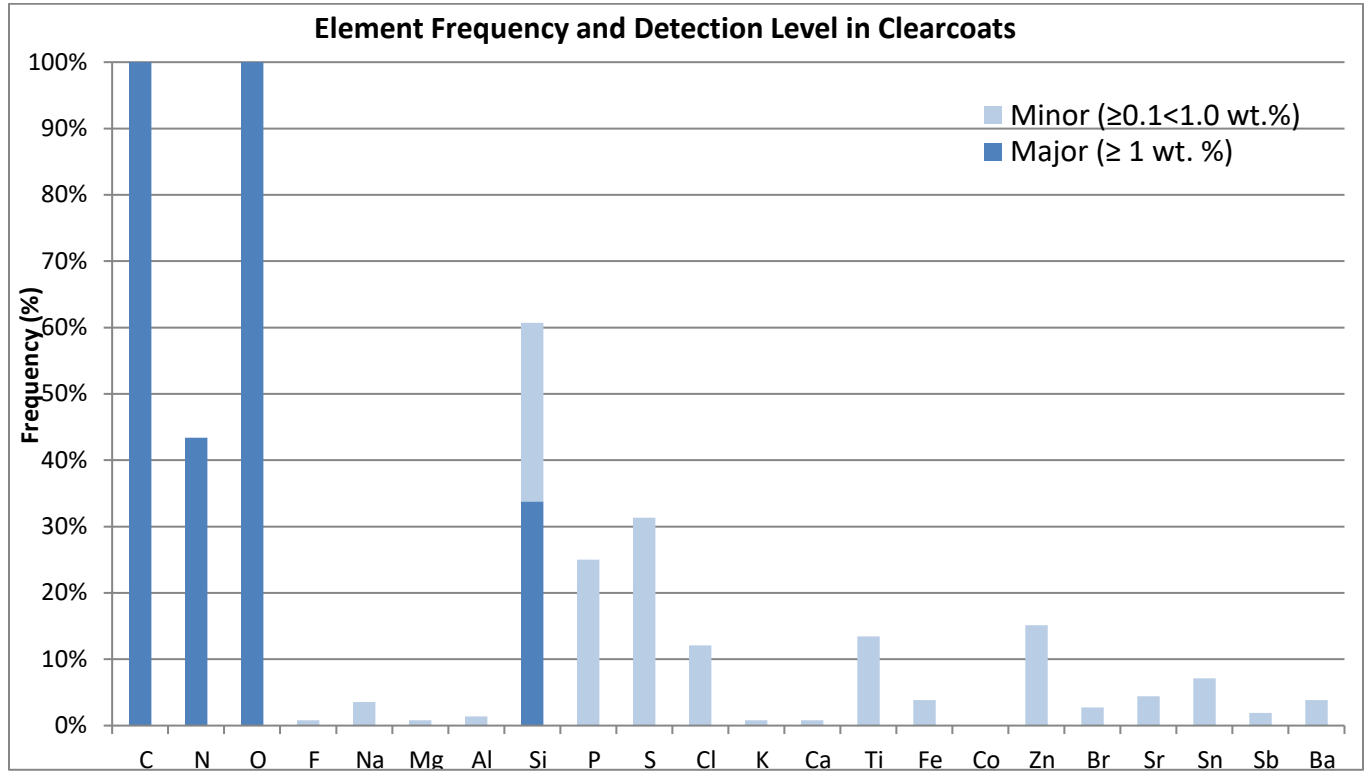


Figure 30. Histogram showing element frequency of occurrence at major and minor concentrations within clearcoat layers.

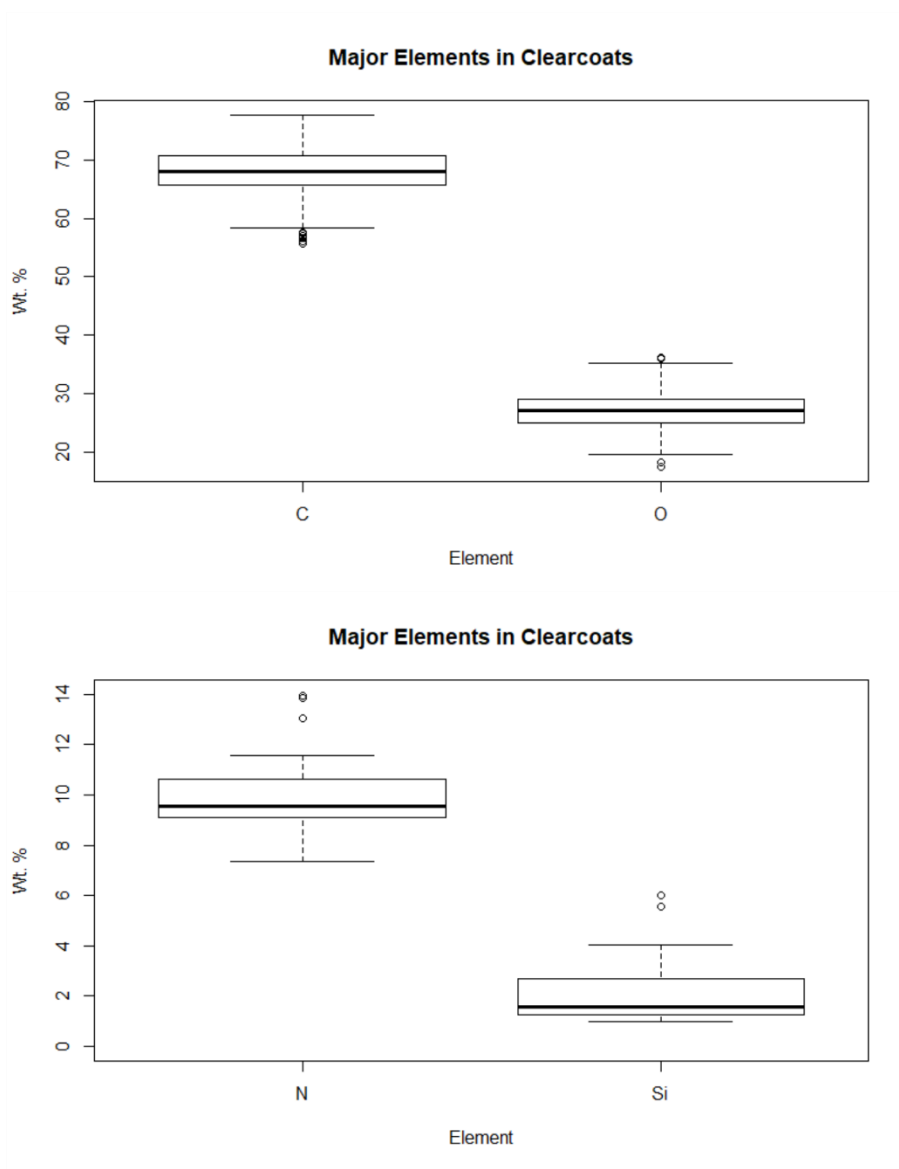


Figure 31. Boxplots showing the most abundance elements observed in clearcoat layers. The region between the upper and lower faces of the boxes contains the middle 50% of the data (interquartile range). The median value for the element is represented by the black.

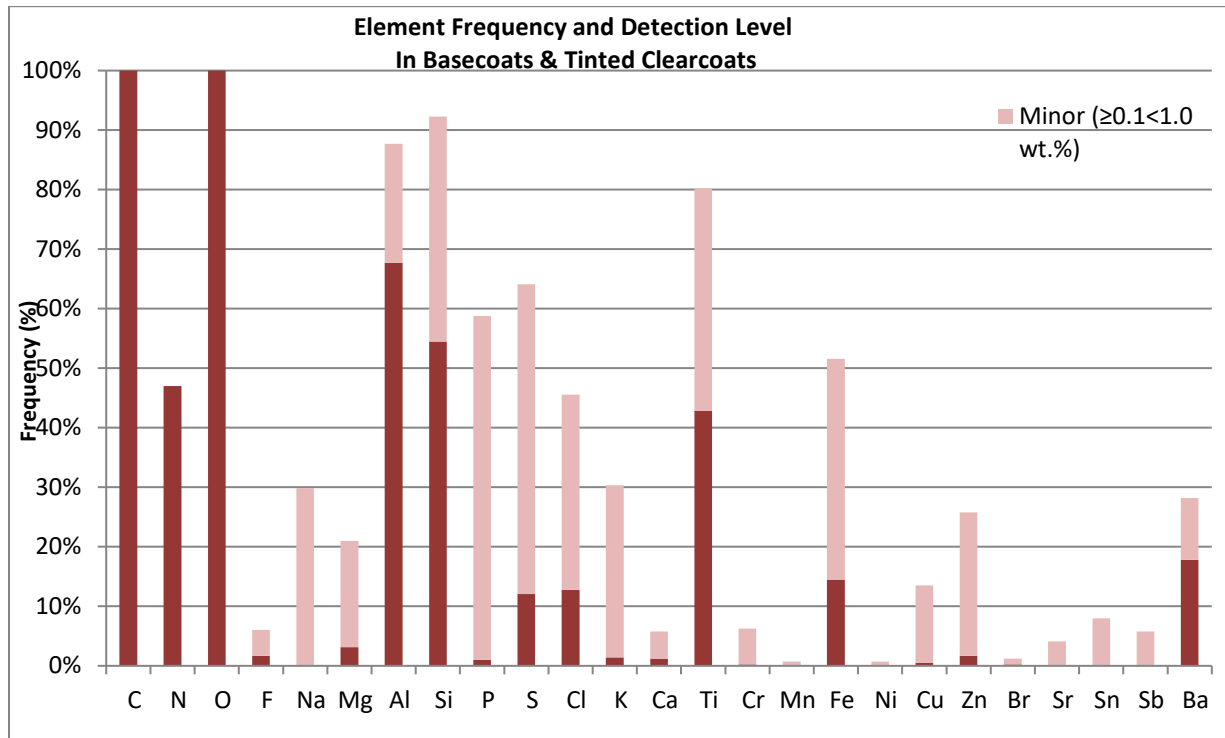


Figure 32. Histogram showing element frequency of detection/ quantitation for the basecoat and tinted clearcoat layers.

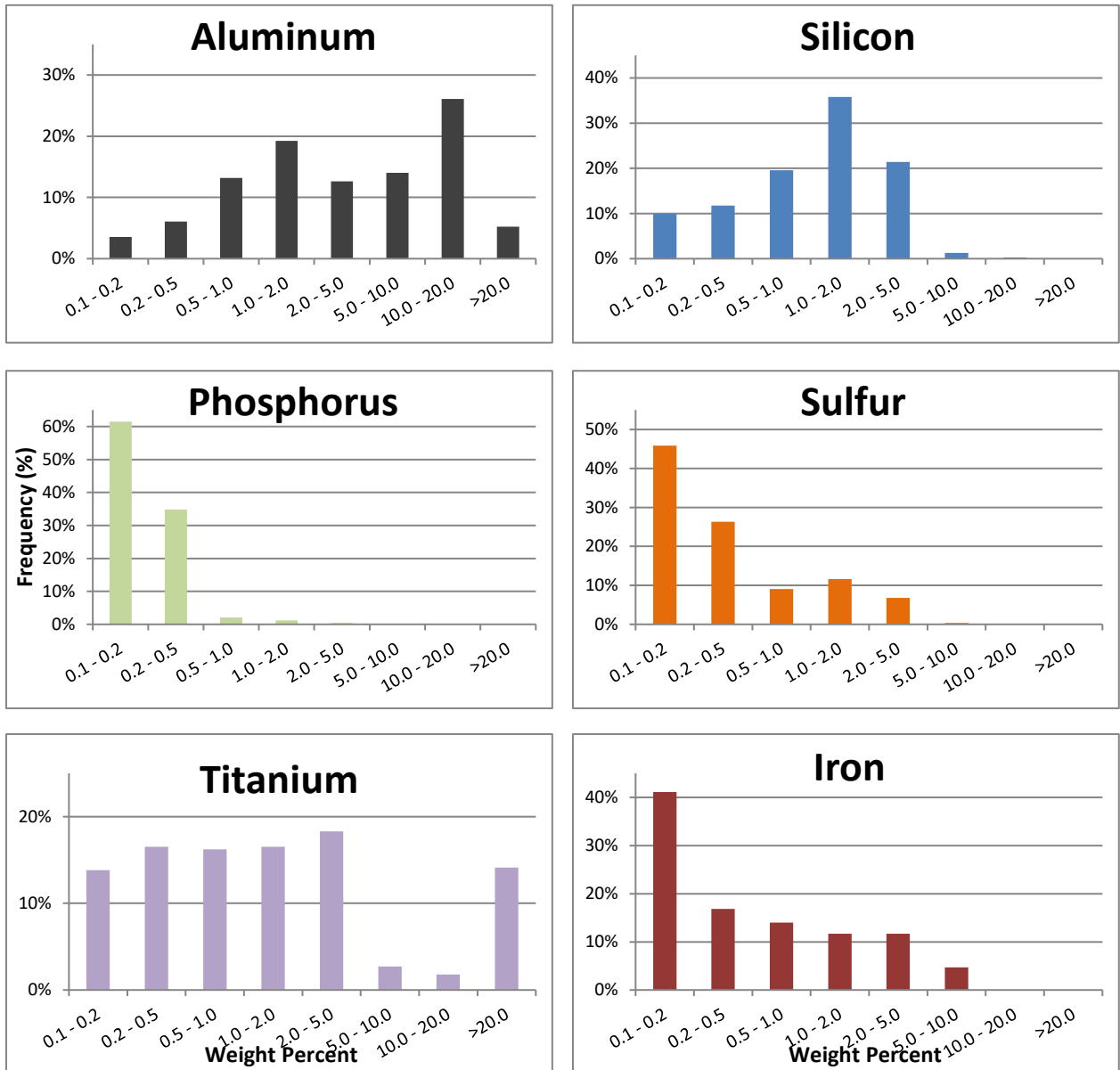


Figure 33. Weight Percent distributions for elements occurring in greater than 50% of the basecoat and tinted clearcoat layers.

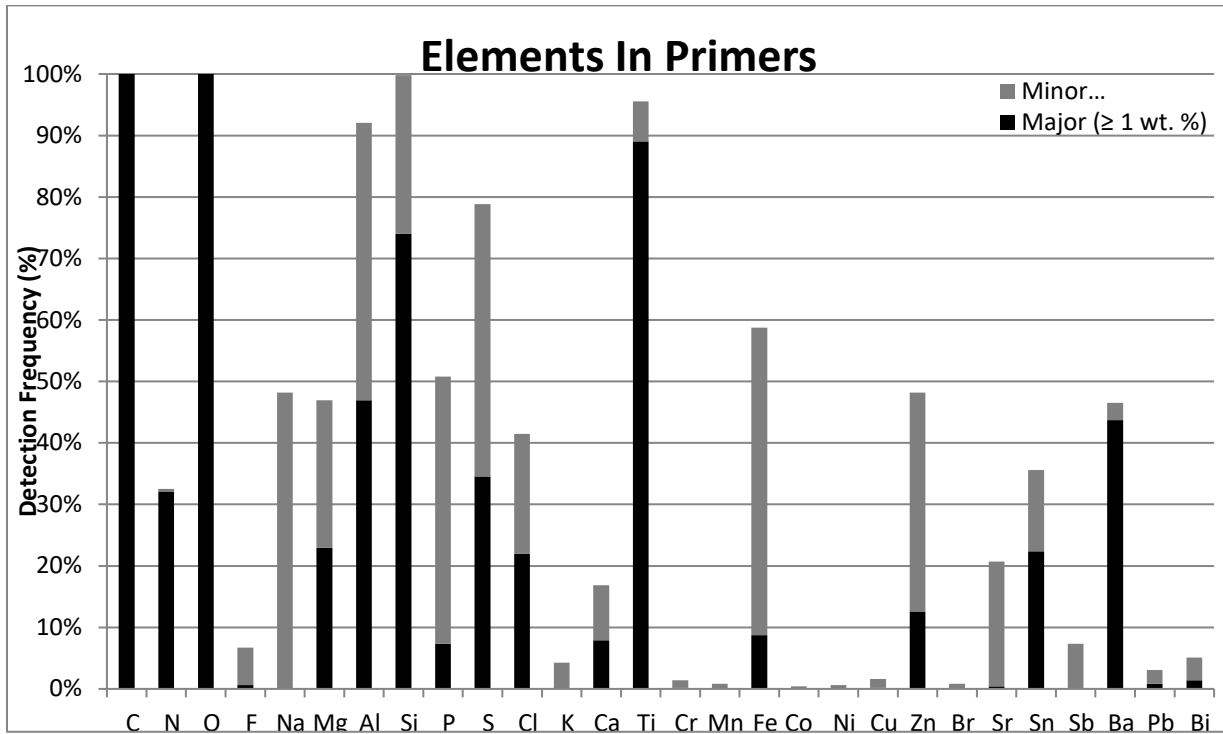


Figure 34. Histogram showing element detection frequency within primer layer.

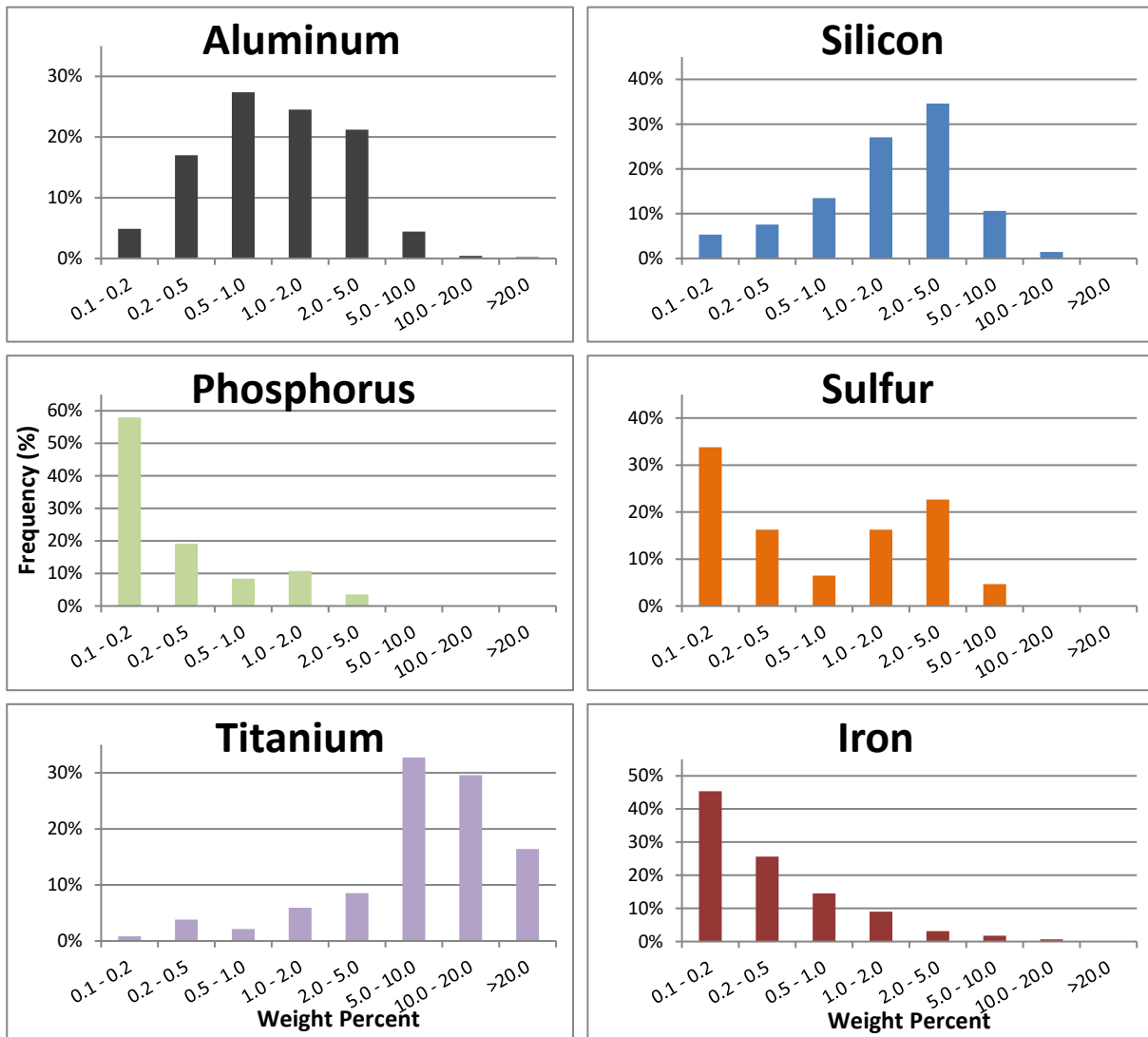


Figure 35. Weight Percent distributions for elements occurring in greater than 50% of the primer layers.

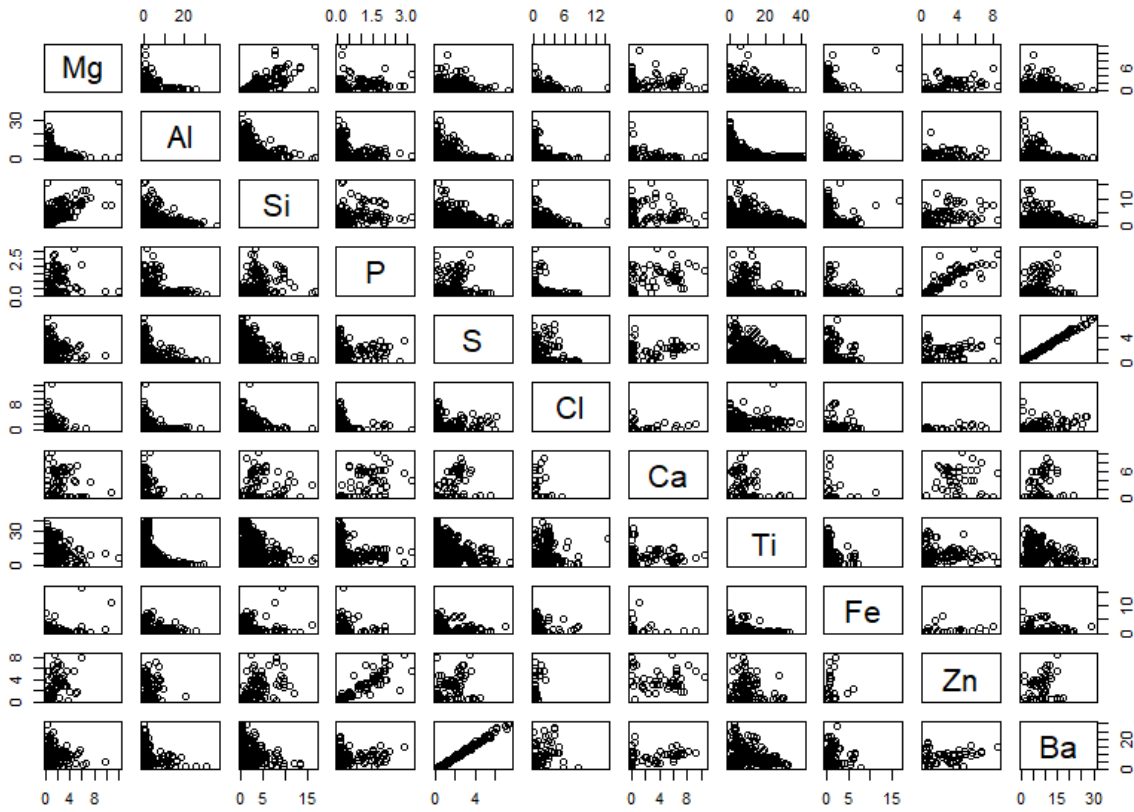


Figure 36. Bivariate plots for eleven selected elements that are most abundant in basecoat and primer layers.

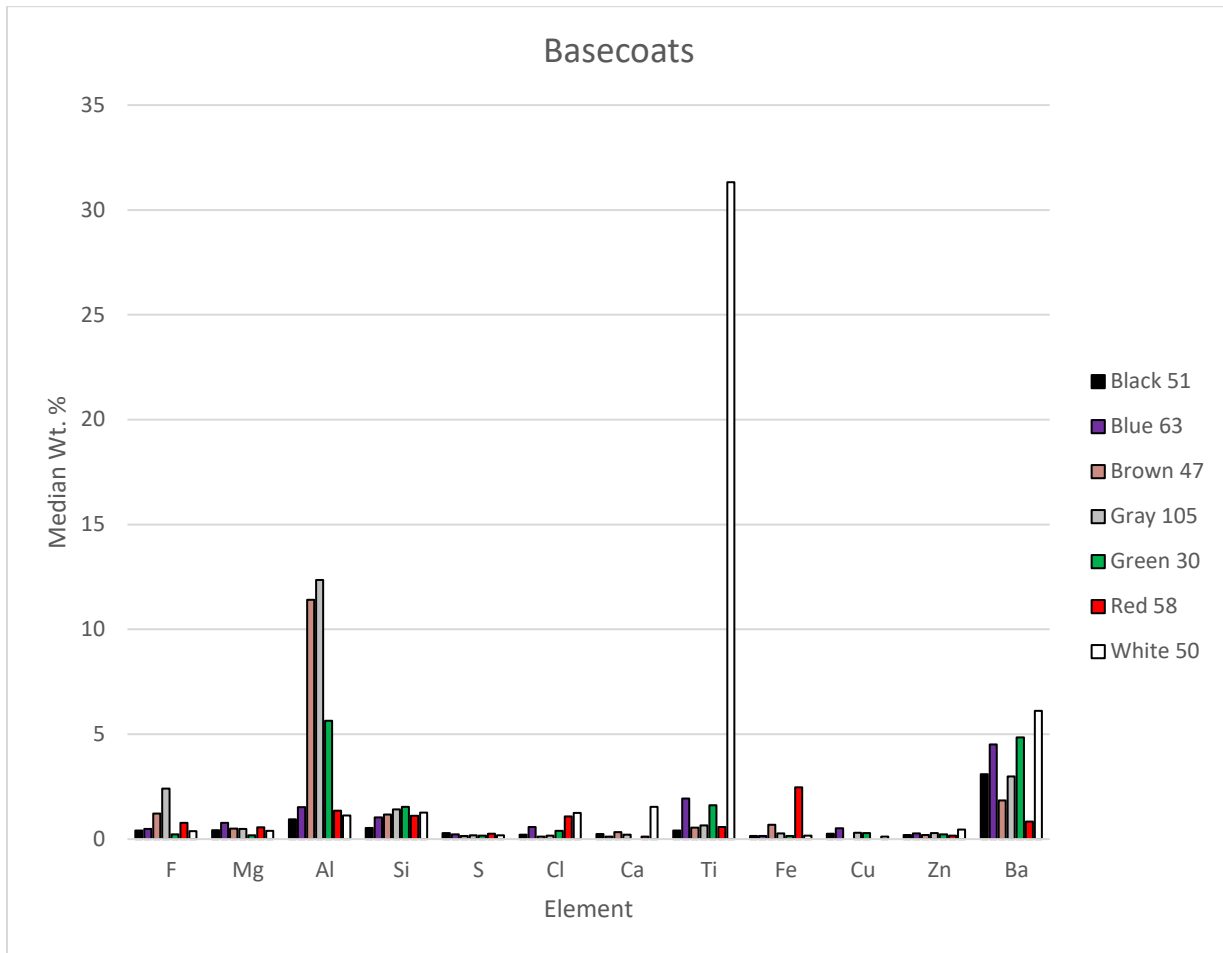


Figure 37. Median element wt. % values for basecoat and tinted clear coat nominal colors.

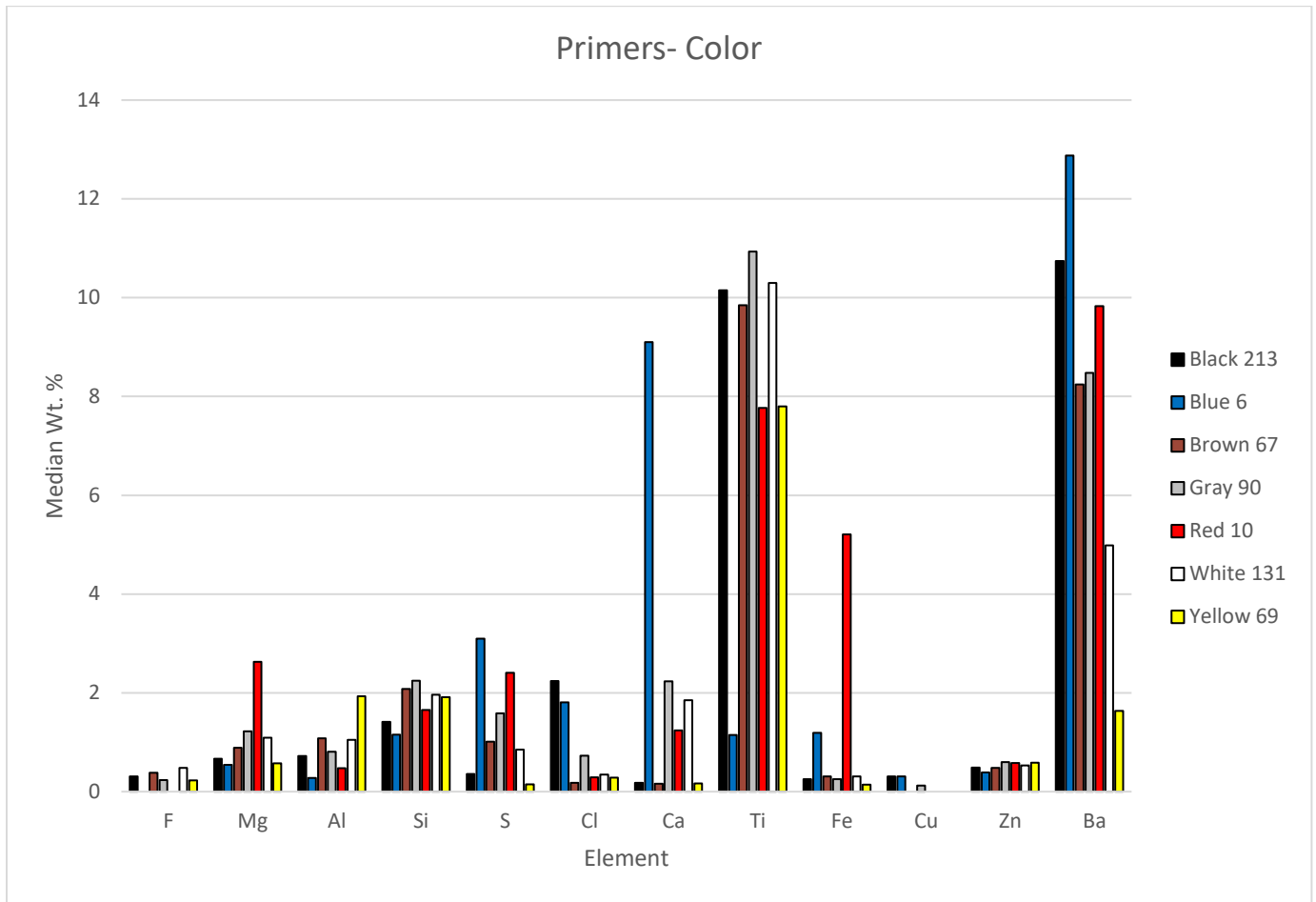


Figure 38. Median element wt. % values for primer and coordinated primer nominal colors.

